WEATHERSMART

NEWS

Scientific meteorological and climatological news from the South African Weather Service

March 2022

Severe thunderstorms cause significant disruptions in parts of Gauteng

The influence of the coastal lows and its effect on the temperatures along the south coast (Western Cape)

Endurance22 expedition and finding the Endurance wreck

South African Weather Service

WEATHERSMART

NEWS

Scientific meteorological and climatological news from the South African Weather Service

Impact-Based Severe Weather Warning System

WHAT IS IMPACT-BASED FORECASTING?

Severe weather is a regular occurrence across South Africa which often negatively affects humans. Due to the vast distribution of vulnerabilities across the country, the same weather hazard can result in different impacts in two areas, depending on the specific vulnerability of the area.

Impact-Based warnings combine the level of impact the hazardous weather conditions expected with the level of likelihood of those impacts taking place

Moving from → **To**

Moving from	To
What the weather will be: (Meteorological thresholds) - 50mm in 24 hours - 35 knot winds	**What the weather will do:** (Impact Warnings) - Roads flooded - Communities cut off

Date of issue:
March 2022

Frequency:
Bi-annual

ISSN:
2414-8644

Compiler and editor: Hannelee Doubell

Publisher:
South African Weather Service
Address:
Eco Glades Block 1B, Eco Park,
Corner Olievenhoutbosch and
Ribbon Grass Streets,
Centurion, 0157

TABLE OF CONTENTS

Foreword by the Chief Executive Officer

It gives me great pleasure as Chief Executive Officer to write the foreword for the March 2022 WeatherSMART News. This publication is now in its seventh year and was started in 2016 to provide a useful publication to the public, where science is made easier for the armchair meteorologist. However, we also publish more complicated scientific articles for those who want a challenge.

This edition covers articles by many of our widely acknowledged scientists: Mr Brighton Mabas summarised a co-authored article as published on www.mdpi.com/2673-7418/1/4/25 giving us an overview of validating hourly satellite-based and reanalyses- based global horizontal irradiance datasets over South Africa. He explains the importance of knowledge about Global Horizontal Irradiance, which is the electromagnetic radiation that reaches the Earth's horizontal surface, especially in terms of assessing ultraviolet effects on health and in the development of a typical meteorological year of a country. I want to encourage you to take the time to read through that article, which has been simplified for readers such as myself.

I am sure many of our readers have heard about forecasts for "Gordonia" in the past. While this could have been a name that has not been used recently, the effect of heay rain in the Gordonia Are of the Northern Cape, brought this remote area under the SAWS radar once again. Gordonia experienced flooding in January 2022, as will be seen in the article "Heavy storms make Gordonia an unforgotten area" and it needs to be emphasized that, for the South African Weather Service, there is no area called "the middle of nowhere, as we are mandated to reach all areas in South Africa and stay in touch with our citizens.

We include an interesting case study about severe thunderstorms that caused disruption in the area south of OR Tambo International Airport (ORTIA) on 26 February 2021. This intense thunderstorm, which can be identified on the radar images in the article, led to flooding and the accumulation of large amounts of small hail at the Alberton hospital as well as the Benoni area. This case study once again shows that thunderstorms can cause notable disruptions in many areas of our day-to-day lives.

Moving to our coastal areas, the article about the "influence of coastal lows and their effect on the temperatures along the south coast" provides a case study about the variation between the forecasted temperature using the different set of models with the observed temperature for 4 March 2020 over the eastern parts of the south coast and to determine how this can be used to improve our forecasting skill for maximum temperatures along the south coast when a coastal low dominates.

We have all seen the media reports about the Endurance22 expedition, where a group of SAWS meteorological scientists joined the group that eventually FOUND the Endurance22 wreck. This is a remarkable achievement and the role of the South African Weather Service Marine Unit in providing on-board weather observations will forever be engraved in the history of this remarkable event.

The article on shock wave effects on readings of South African Automatic Weather Stations (AWS) reveal how two shock waves that were produced by the eruption of the Hunga Tonga volcano were noted on the pressure data of the AWS' of the SAWS. This just once again demonstrates the interlinkage between various geographical occurrences on earth, and how the observations network of SAWS can also be affected by such events.

I would like to thank our contributors for their highly valued articles. The more we do research and produce relevant case studies and articles, the more our understanding of the atmosphere and its atmosphere on Earth will grow.

Please enjoy the wealth of information shared with you in this edition.

Ishaam Abader
March 2022

Validating Hourly Satellite Based and Reanalysis Based Global Horizontal Irradiance Datasets over South Africa

By Brighton Mabasa (taken from an article done by Brighton Mabasa, Meena D. Lysko and Sabata J. Moloi)

Introduction and Background

Solar radiation is the electromagnetic radiation or energy emitted from the surface of the Sun because of the fusion of atoms inside the sun. Global Horizontal Irradiance (GHI) is the electromagnetic radiation that reaches the Earth's horizontal surface after passing through the atmosphere. Accurate knowledge of GHI is important for the technical and economic evaluation of solar energy technologies and in the development and validation of empirical models. Amongst the myriad of applications, GHI is important in climate change and environmental studies, agricultural sciences, hydrology, atmospheric research and in astronomy. GHI is also important in assessing ultraviolet effects on health as well as in material science, and in the development of a typical meteorological year of a country. Therefore, obtaining true solar measurements at a location is important. GHI measurements taken from radiometric stations using at least a good quality (broadband) operational pyranometer remain the most accurate way to collect GHI data. However, GHI monitoring stations are sparse and expensive to install and maintain. As a result, data are only available for a limited number of locations.

Alternative sources of GHI data include models such as the Ångström–Prescott model. Though the model with calibrated coefficients can be used to accurately estimate GHI data, the drawback might be the unavailability of sunshine duration data that are needed as an input at some areas. Another limitation of the Ångström–Prescott model is that the highest possible temporal resolution of estimated GHI is the daily average, so the model is not capable of estimating hourly averages. GHI data can also be generated by interpolation of measured in situ GHI. The drawback of the interpolation method is the biases that are introduced by interpolation, and the additional errors introduced by using sparsely distributed in situ stations. Given that GHI datasets are critical for better understanding of wider coverage of solar radiation, satellite and reanalysis based GHI datasets can be used to provide reliable alternative GHI data and compensate for the scarcity of monitoring stations by increasing the density of GHI data. The satellite or reanalysis-based datasets must first be validated by using GHI data from a good quality pyranometer to obtain proof of their reliability before they are used in different applications.

The satellite based, reanalysis based, and in situ measurements differ in spatial and temporal resolutions. This creates challenges when using satellite based and reanalysis based GHI datasets as alternative GHI sources. To address these challenges, there has been an improvement in the spatio-temporal resolution of satellites and reanalysis-based datasets in the past few years. The improvement was due to the advances in modelling and data assimilation systems. However, there are still challenges due to limited spatio-temporal coverage of observation data in some areas as required by the models.

The algorithms that are used to convert satellite images to estimate GHI data depend on inputs of meteorological parameters (albedo, cloud thickness, aerosols, water vapor, and ozone content). When the parameters have not been measured in some areas, estimated or monthly climatologies are used. Climatological values might not fully represent changes in atmospheric constituents, and as a result, introduce errors in the estimated GHI data when used as inputs.

This study aimed to contribute to the reviewed literature by validating satellite-based datasets (SOLCAST, CAMS, and CMSAF SARAH) and reanalysis-based datasets (ERA5 and MERRA2) relative to quality controlled in situ data from 13 reference stations managed by the South African Weather Services (SAWS). The validation was conducted on an hourly temporal scale over all six macro climatic zones of South Africa.

Validated datasets could be used to estimate GHI in the long-term and over a wide spatial resolution in South Africa. This will enable climate studies, which is generally not possible with ground observed data because there are no continuous long-term records covering decades and covering all areas of the country. The validated datasets could also be used as an additional quality control parameter of the measured data. The bias information from different sources of GHI in different areas of the country can be used as a basis for bias correction. The bias corrected data sources could also be merged with measured in situ data by applying interpolation with external drift kriging to produce most accurate GHI maps than when using an individual data source.

2. Data and Methodology

The study area was determined by considering the location of South African Weather Service (SAWS) radiometric network of 13 stations that are distributed in all six macro-climate regions in South Africa (with location and climate as shown in Figure 1 and given in Table 1).

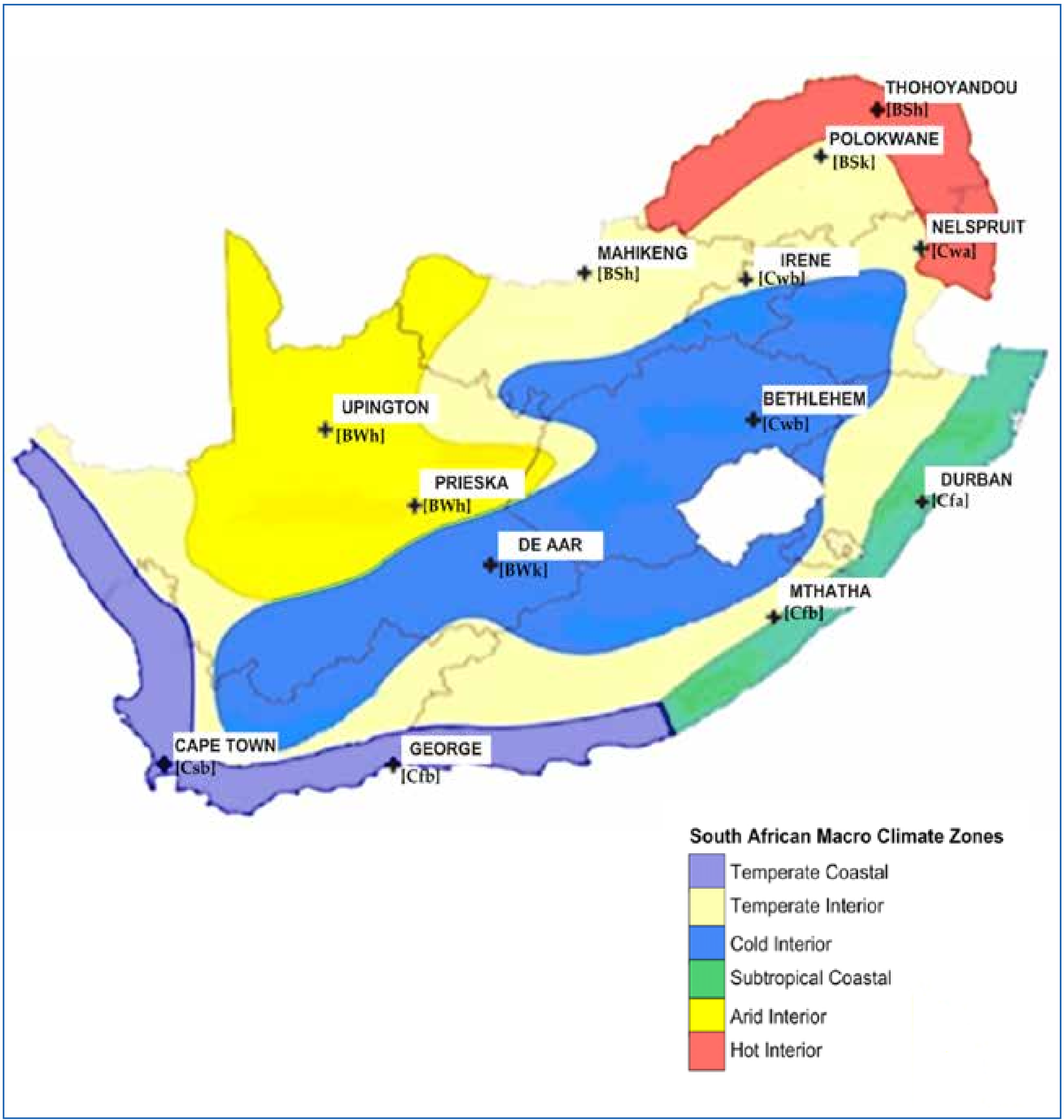

Figure 1: A map showing the location of the South African Weather Service's radiometric station, SAWS macro climate zones

Table 1: South African Weather Services radiometric stations with Köppen–Geiger climate classification (KGCC), altitude, latitude, climatic zones, average number of clear sky days per year (percentage of clear sky days per year), annual aggregated diffuse fraction, humidity, and the percentage of data outliers removed per station.

Station	KGCC	Altitude (m)	Latitude (°)	GHI Observation Period	Clear sky days	Diffuse Fraction	Humidity	Outliers (%)
Upington	BWh	848	−28.48	2014-02-01 to 2019-11-30	97 (27)	0.18	35.4	4.47
Prieska	BWh	989	−29.68	2013-09-01 to 2015-08-31	78 (21)	0.18	38	3.88
De Aar	BWk	1284	−30.67	2014-05-01 to 2019-12-31	58 (16)	0.2	44.5	4.23
Bethlehem	Cwb	1688	−28.25	2015-01-01 to 2019-12-31	43 (12)	0.31	59.1	6.57
Irene	Cwb	1524	−25.91	2014-03-01 to 2019-12-31	62 (17)	0.3	54.9	2.99
Mahikeng	BSh	1289	−25.81	2016-01-01 to 2019-12-31	77 (21)	0.24	43.9	6.4
Polokwane	BSk	1233	−23.86	2015-03-01 to 2019-12-31	49 (13)	0.31	58.2	5.12
Nelspruit	Cwa	870	−25.39	2014-02-01 to 2019-12-31	39 (11)	0.4	62	5.85
Thohoyandou	BSh	619	−23.08	2015-03-01 to 2017-10-31	50 (14)	0.34	60.8	4.06
Mthatha	Cfb	744	−31.55	2014-07-01 to 2019-12-31	19 (5)	0.33	68.1	4.98
Durban	Cfa	91	−29.61	2015-03-01 to 2019-12-31	20 (5)	0.39	72.8	5.34
Cape Point	Csb	86	−34.35	2015-02-01 to 2019-12-31	12 (3)	0.34	77.2	4.96
George	Cfb	192	−34.01	2015-01-01 to 2019-12-31	11 (3)	0.36	79.2	2.75

2.1 Description of validated data sources

Data	Data derived from	Time Period	Spatial Resolution	Temporal Resolution	Data Availability	Region Available
SOLCAST	satellite	2007 to present	1–2 km	1 hour	Not free	Almost Global (except Polar regions and oceans)
CMSAF SARAH	satellite	1983 to present	0.05° x 0.05° (5 km)	½ hour, 1 day	Free	Europe, Africa, and a small part of South America
CAMS	satellite	2004 to (current day - 2 days)	*Interpolated to a point of interest	1 minute, 15 minutes 1 hour, 1 day, 1 month	Free	Europe, Africa, Middle East, Eastern part of South America and Atlantic Ocean
ERA5	reanalysis	1979 to present	0.25° x 0.25° (31 km)	1 hour	Free	Global
MERRA2	reanalysis	1980 to (present—2 months)	0.625° x 0.5° (50 km)	1 hour	Free	Global

2.2 Methodology

The methodology used in this study is summarized in the flow chart in Figure 2.

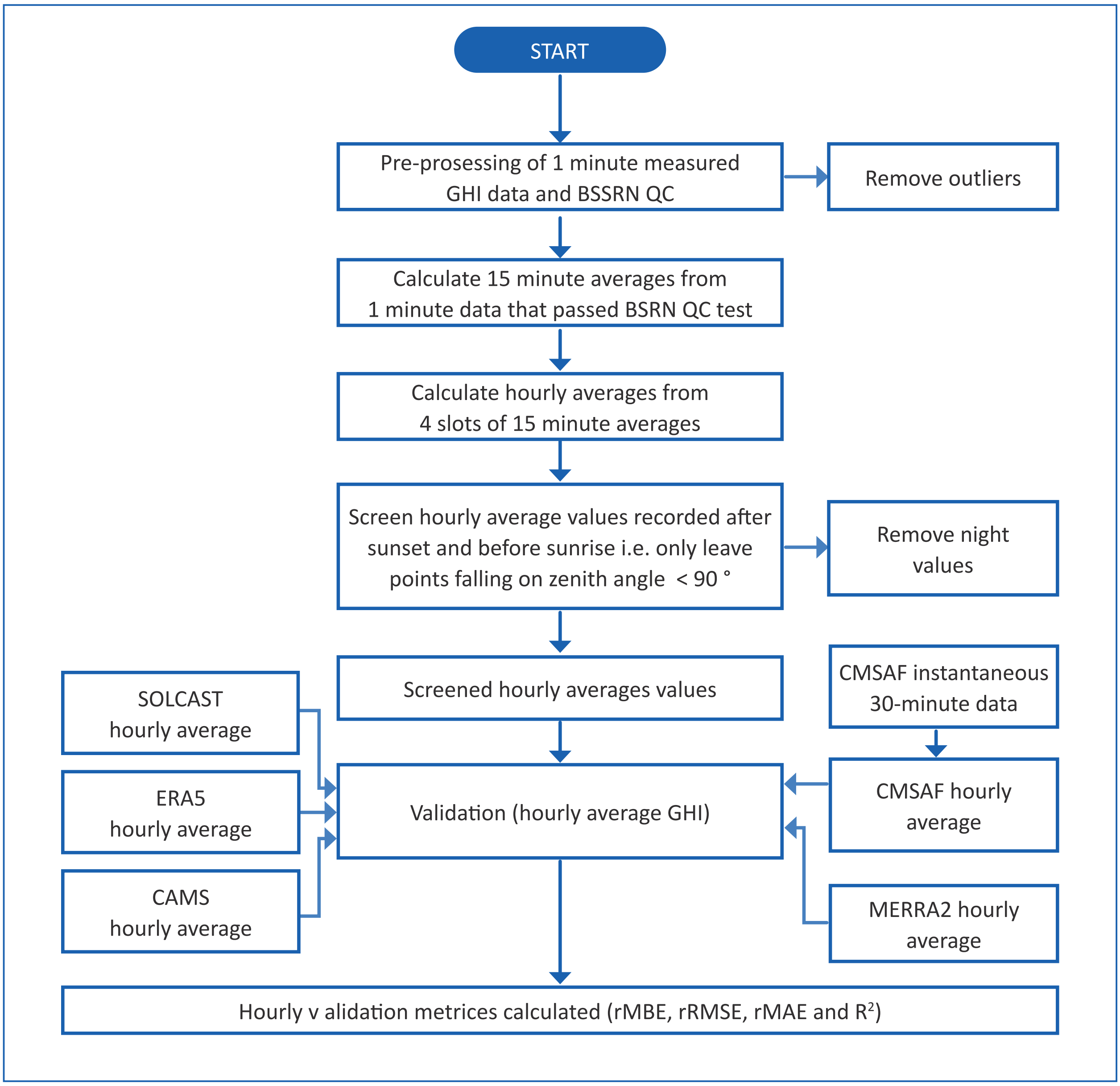

Figure 2: The flowchart summarizes the approach used from data prepossessing to data validation.

3. Results and Discussions

The statistical metrics results suggest that the CAMS dataset has good performance in South Africa and can therefore be used with quantitative confidence as a reliable alternative source of estimated GHI data. The relatively high rRMSE observed for Nelspruit, Thohoyandou, Mthatha, Durban, Cape Point, and George may be due to the characteristic high annual humidity (greater than 60% in Table 1), George and Nelspruit stations also had a high diffuse fraction (DF > 0.32). This implies that the performance of CAMS is affected by high aerosols, high humidity, and hence, many days with diffuse skies. When considering areas where there is infrequent cloud occurrence, there was no significance difference in bias, meaning that McClear can accurately estimate clear sky conditions in the study area.

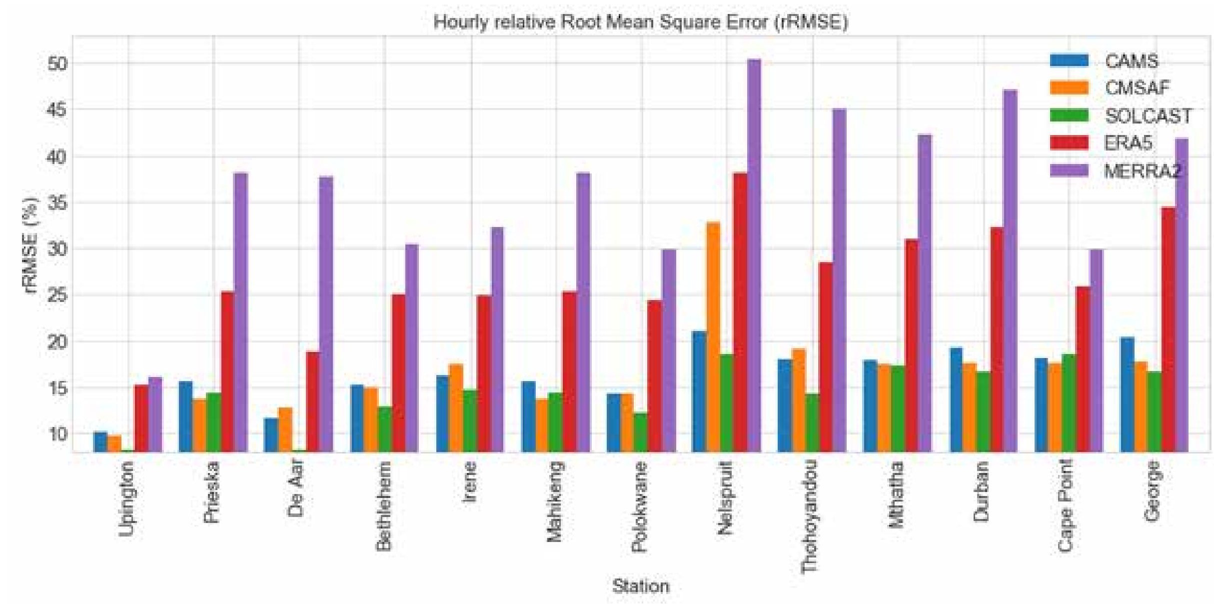

Figure 3: Hourly relative root mean square error of gridded datasets against measured in situ GHI.

Table 2: Best performing gridded dataset per hourly metric, most feasible model, and level of performance (rating). The colors were used to show the best performing gridded dataset based on the hourly statical metric per station and the most feasible dataset per station based level of rating out of 4 (the number of statistical metrics used). Green represents SOLCAST, yellow CAMS, blue CMSAF, orange ERA5, and red MERRA2.

Hourly	Minimum rMBE	Minimum rRMSE	Minimum rMAE	Maximum R^2	Most Feasible	Rating
Upington	SOLCAST	SOLCAST	SOLCAST	SOLCAST	SOLCAST	4/4
Prieska	CAMS	CMSAF	SOLCAST	SOLCAST	SOLCAST	2/4
De Aar	ERA5	SOLCAST	SOLCAST	SOLCAST	SOLCAST	3/4
Bethlehem	CMSAF	SOLCAST	SOLCAST	SOLCAST	SOLCAST	3/4
Irene	ERA5	SOLCAST	CAMS	SOLCAST	SOLCAST	2/4
Mahikeng	MERRA2	CMSAF	CMSAF	CMSAF	CMSAF	3/4
Polokwane	ERA5	SOLCAST	SOLCAST	SOLCAST	SOLCAST	3/4
Nelspruit	ERA5	SOLCAST	SOLCAST	SOLCAST	SOLCAST	3/4
Thohoyandou	SOLCAST	SOLCAST	SOLCAST	SOLCAST	SOLCAST	4/4
Mthatha	SOLCAST	SOLCAST	CAMS	CMSAF	SOLCAST	2/4
Durban	SOLCAST	SOLCAST	SOLCAST	SOLCAST	SOLCAST	4/4
Cape Point	CAMS	CMSAF	SOLCAST	CMSAF	CMSAF	2/4
George	SOLCAST	SOLCAST	SOLCAST	SOLCAST	SOLCAST	4/4

The overall CMSAF results show that there is relatively good performance in South Africa, which suggests that CMSAF is a viable tool to estimate GHI for sites such as the 13 stations in this study. CMSAF satellite-based dataset showed a relatively poor performance at Nelspruit Station. Nelspruit is a station with the highest diffuse fraction (Table 1). CMSAF satellite-based dataset uses aerosol climatology as input to satellite retrieval algorithms as given by Riihelä et al. [49], however, aerosol climatology might not capture the aerosol climate variability. Mueller et al. [54] showed that aerosol climatologies used in CMSAF satellite retrievals algorithms were underestimated when compared to real aerosol measurements. The poorer metrics for Nelspruit might be due to the use of aerosol climatology information in the CMSAF satellite retrieval algorithm.

The overall SOLCAST results show that there is a relatively very good performance in all 13 stations in this study. Overall SOLCAST was outperformed by CMSAF (from Table 2) at Mahikeng and Cape Point stations; meaning SOLCAST did not outperform some freely available products at all sites. The stations where rRMSE was greater than 15% when referencing from Tables 1. They all had a low number of clear sky days (less than 5%), high humidity (greater than 60%), and high diffuse fraction (greater than 0.33), except Nelspruit Station with (more than 10%) number of clear sky days. This implies that frequent cloud occurrence, higher humidity, and higher diffuse fraction slightly affected the performance of the SOLCAST satellite-based dataset. The excellent performance of the SOLCAST dataset might be due to the use of the REST2v5 [45] clear sky model to calculate the clear sky index when converting the satellite image to GHI. Sun X et al. [56] found that the REST2v5 clear sky model had an excellent worldwide performance. The use of very high spatial resolution satellite images 1–2 km enabled almost all features (e.g., terrain difference) in an area of interest or a grid to be properly identified and properly interpolated.

Overall, the ERA5 and MERRA2 reanalysis dataset showed a poor performance in estimating GHI in South Africa. Raanalysis datasets showed a very poor performance in areas with frequent cloud occurrences, high humidity, and high diffuse fraction. Basically, ERA5 and MERRA2 cloud models struggle to differentiate non cloud and cloud conditions. The low spatial resolution of ERA5 (0.25° x 0.25°) and MERRA2 (0.625° x 0.5°) might also be a contributing factor to poor performance of reanalysis datasets.

4. Conclusions

The study validated hourly global horizontal irradiance (GHI) from three satellite-based GHI datasets (namely SOLCAST, CAMS, and CMSAF SARAH) and two reanalysis based GHI datasets (namely ERA5 and MERRA2) against quality-controlled hourly in situ GHI recorded at 13 radiometric stations in South Africa. The study demonstrated that GHI from the satellite-based datasets had better performance than reanalysis-based datasets in South Africa. SOLCAST was the best performing overall, while MERRA2 was the overall worst performing dataset. Freely available satellite-based datasets (CAMS and CMSAF) are recommended for use with quantitative confidence in diverse solar energy applications that require GHI data. Reanalysis based GHI datasets (ERA5 and MERRA2) are not good enough to be used in South Africa. Low spatial resolution, weak cloud parameterization schemes, and the use of climatological inputs instead of real in situ measurement in reanalysis GHI deriving algorithms might be some of the reasons behind the poor performance of reanalysis based GHI estimates in the study.

Source : https://www.mdpi.com/2673-7418/1/4/25

Heavy Storms Make Gordonia an Unforgotten Area

By Puseletso Mofokeng and Lesetja Lekoloane

The scope of weather and climate services offered by the South Africa Weather Service (SAWS) is indiscriminate and there is no exclusive loyalty to popular cities such as Johannesburg, Pretoria, Durban or Cape Town, to name a few. The mandate of the national provider of weather and climate services extends from the big cities to small towns of the Republic, in no particular order.

There should not even be a single forgotten village. An example is an alert issued by SAWS to "remote areas" such as Gordonia in the Northern Cape Province. On 19 January 2022, there were semi-stationary multicell thunderstorms (Figure 1) which threatened Groot Mier with flooding, located within the ZF Mgcawu District Municipality. This occured during the early evening of Wednesday, 19 January 2022, and brought "remote areas" such as Gordonia back into the equation. The Gordonia area is susceptible to flooding due to the soil in this area largely being dry with relatively flat landscape. It should not be an after-thought that Kgalagadi Transfrontier Park in the northern-most parts of the Northern Cape hosts wild animals some of which may not survive all harsh weather conditions. On the aftermath of extreme thunderstorms, conservationists often find the rehabilitation of vegetation necessary.

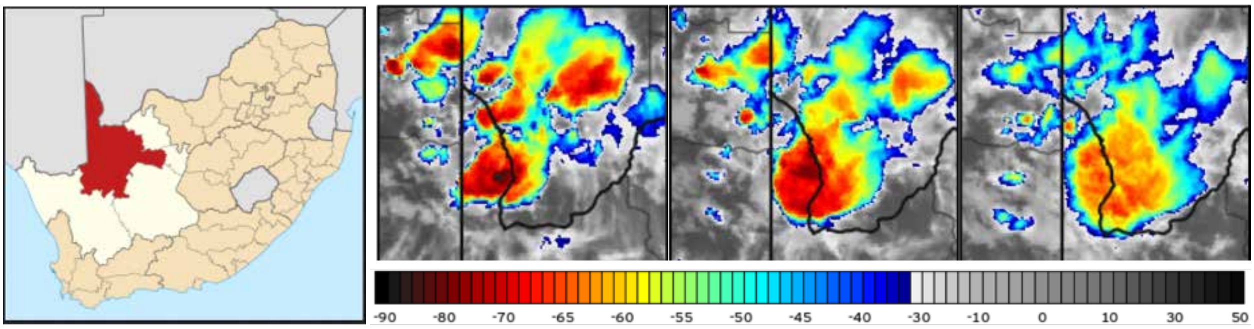

Figure 1: (a) South Africa map indicating ZF Mgcawu district municipality (red shade) where Groot Mier and Gordonia are located. Images of multicell thunderstorms in the district area on 19 January 2022 are also indicated by infrared satellite with cloud top temperatures (in °C) at (b) 19:30, (c) 20:30 and (d) 21:30.

The SAWS is compelled to pay full attention to heavy storms despite their lifespan. For example, heavy winds with risk of damage to roofs, other properties and shrubs could not be ruled out after two hours of the intense storm – from about 21:15 through 21:30 (Figure 1 (d)). The anticipation for such wind impacts stems from the acceptance that the rapid demise of the multicell thunderstorms is associated with enhanced downbursts. However, a direct evidence of the impacts of storms such as these in "remote areas" is hard to come by, consequential of very slow economic activities and internet speed, low or non-existent media coverage including in social media front.

Regardless of whether these communication hurdles are regarded insurmountable or not, SAWS is mandated to reach all areas in South Africa and is so in touch with citizens; there is no area called the *"middle-of-nowhere"*.

Severe thunderstorms cause significant disruptions in parts of Gauteng

By Hetisani Oscar Shiviti

A thunderstorm is primarily a storm that is accompanied by thunder and lightning. In the aviation industry a thunderstorm is significant because of the many different hazards which can be associated with the cumulonimbus cloud and/ or the thunderstorm. One distinction to make is that thunderstorms always occur in the presence of a cumulonimbus; whereas cumulonimbus clouds do not always occur with thunderstorms (the clouds can exist without a thunderstorm occurring).

There are three types of thunderstorms, namely a single cell thunderstorm, a multi-cell thunderstorm and a supercell thunderstorm. For aviation purposes, a thunderstorm is always considered a significant phenomenon because of the presence of the following hazards:

- Heavy precipitation leading to poor visibility
- Electrical phenomena
- Microburst or gust fronts
- Associated tornadic activity
- Moderate and/ or severe turbulence
- Moderate and/ or severe in-flight icing
- Associated hail

It is important to note that the above-mentioned do not always have to happen all at once, however, the presence of just one of them can have a significant negative impact on aviation.

In South Africa, thunderstorm activity usually occurs during summer seasons, however, it is possible for thunderstorms to develop outside of the summer season depending on the atmospheric systems driving the weather. Thunderstorms can also cause notable disruptions for the transport industry, mainly as they can have considerable impacts on visibility, surface-level and upper-level winds.

On 26 February 2021, severe thunderstorm activity developed south of OR Tambo International Airport (ORTIA), which resulted in significant disruptions to communities in the area. From Figure 1 below, the thunderstorms can be identified by well-defined “deep cyan clumpy clouds”. In Figure 1A it can be seen that at 0800Z (10:00 SAST) thunderstorm development was only over the south-eastern parts of Gauteng; two hours later (12:00 SAST), storm development had spread further north-west and storms were now over the central and eastern parts of Gauteng as can be seen in Figure 1B; a further two hours later (14:00 SAST), thunderstorms were seen covering the whole of Gauteng (Figure 1C).

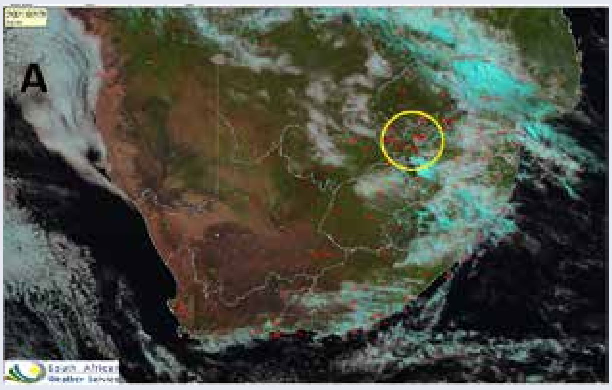

(a)

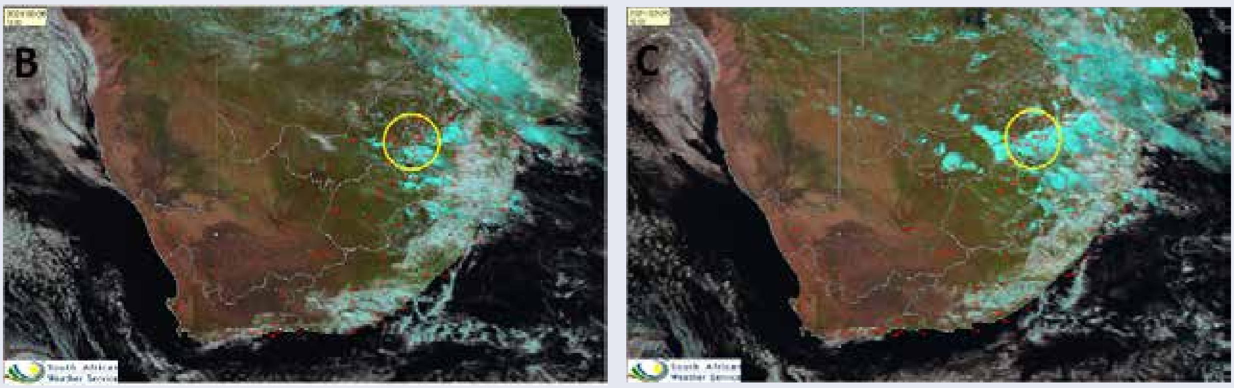

(b) (c)

Figure 1: Day Natural Colours (DNC) satellite imagery showing thunderstorm development and movement over Gauteng on 26 February 2021. (SAWS and EUMETSAT)

To show the intensity of the respective thunderstorms moving over Gauteng on 26 February 2021, radar imagery is investigated for similar times as those used for the satellite imagery as can be seen in Figure 2 below. All radar images are provided with a legend on the right-hand side of the image; the legend is colour coded and indicates how high the maximum dBZ (decibel) of a thunderstorm is – the higher the maximum dBZ, the more intense the thunderstorm is. Thunderstorms on the radar image can be identified by the brightly coloured cells.

In Figure 2A the radar imagery is in support of the satellite imagery that at 0759Z (09:59 SAST) thunderstorm development was only over the south-eastern parts of Gauteng. At this time thunderstorms had a maximum dBZ of 54. At 1004Z (12:04 SAST) the thunderstorm cells had moved to just south of the OR Tambo aerodrome (this can be spotted by the blue circular ring, with the Lanseria aerodrome located north-west of it) – the size and intensity of the thunderstorms had increased with the maximum dBZ at this time observed to be 68 dBZ as can be seen in Figure 2B. At 11:58Z (13:58 SAST) the thunderstorms had continued to move further north over Gauteng and were now north of OR Tambo Aerodrome; at this time the max dBZ varied between 42 and 64 dBZ as can be seen in Figure 2C.

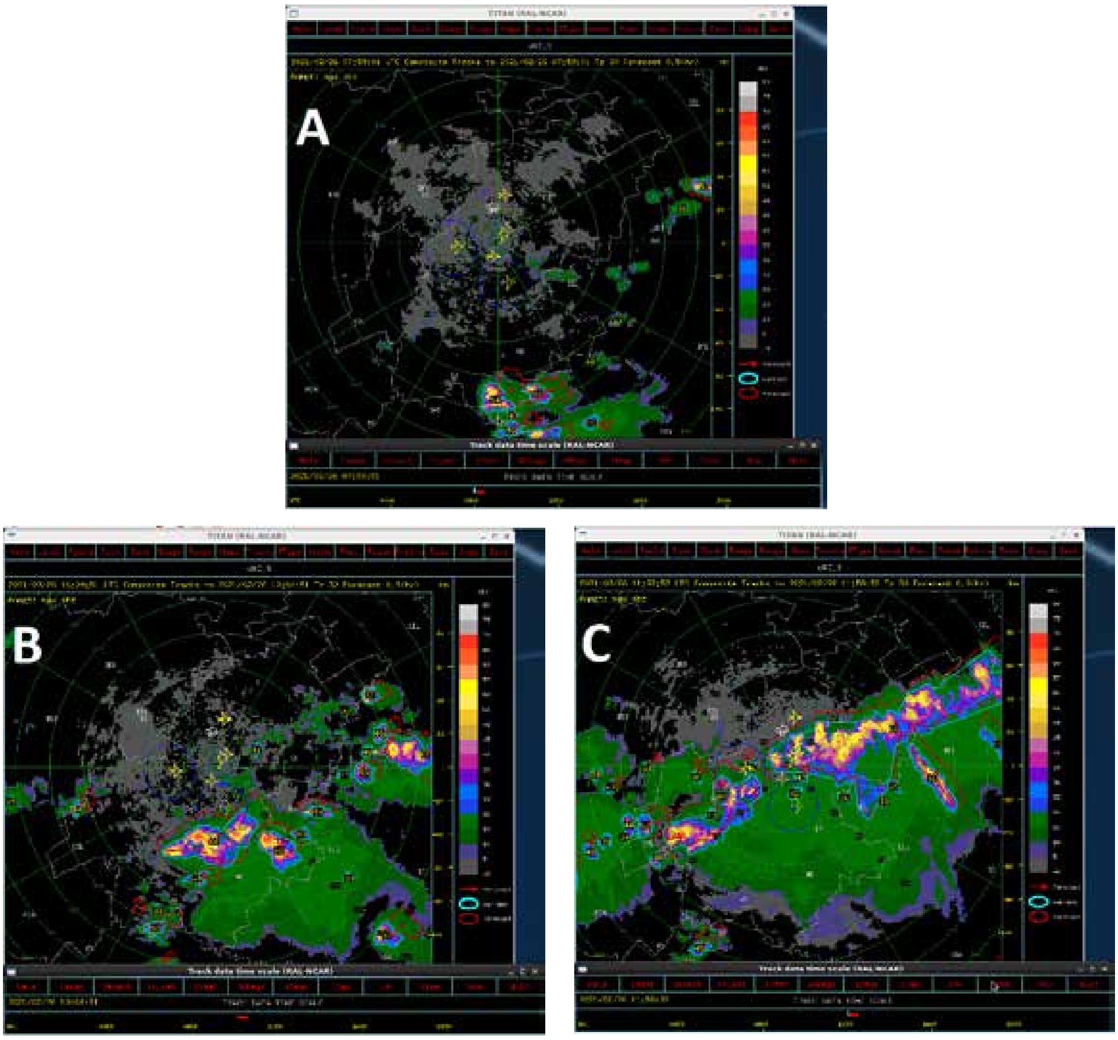

Figure 2: Radar imagery showing thunderstorm development, intensity and movement over Gauteng on 26 February 2021. *(SAWS)*

From both the satellite and radar imagery it can clearly be deduced that the thunderstorms moved over the OR Tambo Aerodrome between 1000Z and 1200Z (between 12:00 and 14:00). Meteorological Aerodrome Reports (METARs) for surface observations at OR Tambo International Airport between 1000Z and 1100Z (between 12:00 and 13:00) on 26 February 2021 can be seen in Figure3. At 1100Z (13:00) the conditions were so bad that visibility had dropped to 1500 meters due to the heavy thunderstorm and rain with small hail, which can clearly be seen highlighted in red in Figure 3.


Station: FAOR

Date: 2021-02-26

COR FAOR 261630Z 12005KT 060V170 9999 SCT020 17/14 Q1020 NOSIG=

FAOR 261000Z 36008KT 290V030 9999 TS BKN030 FEW035CB 23/15 Q1020 TEMPO 3000 TSRAGS=

FAOR 261030Z 16015G25KT 140V220 9999 5000SE -TSRA FEW012 BKN030 FEW035CB 18/13 Q1020 TEMPO 1200 +TSRAGS=

FAOR 261030Z 16015G25KT 140V220 9999 5000SE -TSRA FEW012 BKN030 FEW035CB 18/13 Q1020 TEMPO 3000 TSRAGS=

FAOR 261100Z 12010KT 080V190 1500 +TSRAGS FEW010 BKN030 SCT035CB 14/11 Q1022 BECMG 4500 TSRA FEW035CB=

Figure 3: Meteorological Aerodrome Reports (METAR) at OR Tambo International Airport between 1000Z and 1100Z on 26 February 2021. (SAWS)

Because of the severity of the impacts caused by thunderstorms on 26 February 2021, there were a lot of observations by individuals in different parts of Gauteng. In Alberton, flooding of parking lots was observed due to the heavy rain as seen in Figure 4A, while flooding as well as accumulation of large amounts of small hail was observed at the Netcare Union Hospital in Alberton which can be seen in Figures 3B and 3C.

Figure 4: Flooding as well as accumulation of large amounts of small hail observed at the Alberton hospital on 26 February 2021. (Courtesy of @crimeairnetwork (REZA))

In Benoni, large amounts of small hail were observed - see Figure 5A, which also disrupted the traffic on the N12 in Benoni (Figure 5B).

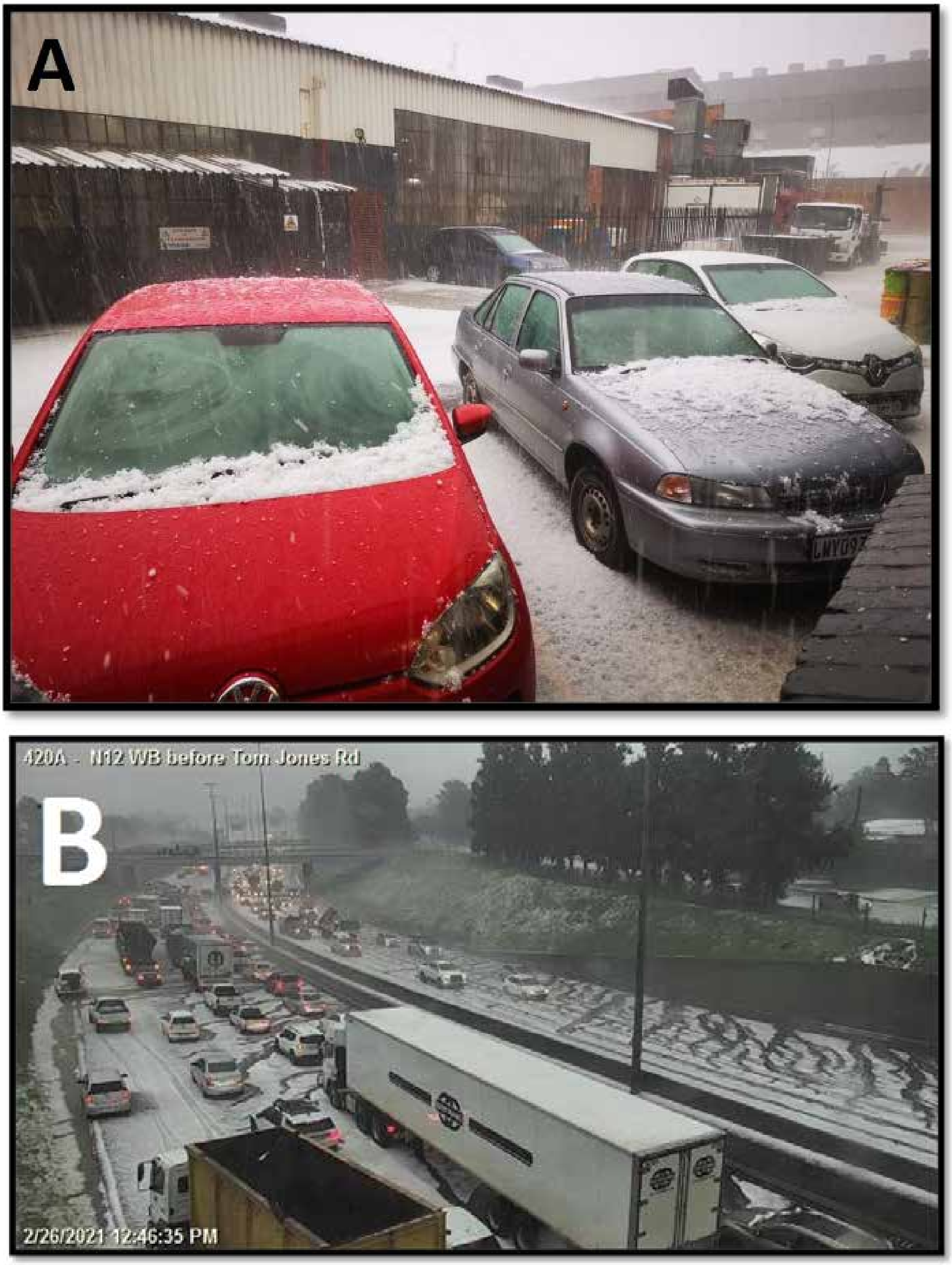

Figure 5: Large amounts of small hail observed falling on top of cars in Benoni on 26 February 2021. (Courtesy of @SAWeatherServic (SA Weather Service))

The influence of coastal lows and their effect on the temperatures along the south coast (Western Cape)

By Samkelisiwe Thwala

A coastal low is a shallow cyclonic (usually not deeper than 850 hPa) mesoscale weather system which originates along the west coast of Southern Africa and propagates southwards and thereafter eastwards along the south coast. This system is associated with warm offshore air ahead and cool onshore flow behind it, resulting in warm continental air descending from the escarpment to the sea which is later replaced by cooler maritime air. Coastal lows owe their existence to the patterns of the escarpment, plateau and the coastal orientation and can lead to the formation of light precipitation such as drizzle and mist or fog conditions over the coastal regions. This system is usually associated with berg winds (berg winds are a hot dry winds that originate from the interior and are characterised by a sharp increase in temperature). A low-level inversion is usually associated with the coastal low as the inversion usually extends to approximately the height of the topography.

On 4 March 2020, there was a coastal low that was situated over the west coast of the Western Cape, which propagated eastwards along the south coast. With this system clear skies with fine weather conditions were expected with fairly warm temperatures reaching a maximum of about 30°C. However, an early maximum temperature occurred which was approximately 8°C higher than forecast and 11°C higher than the Unified Model Temperature Forecast (corrected).

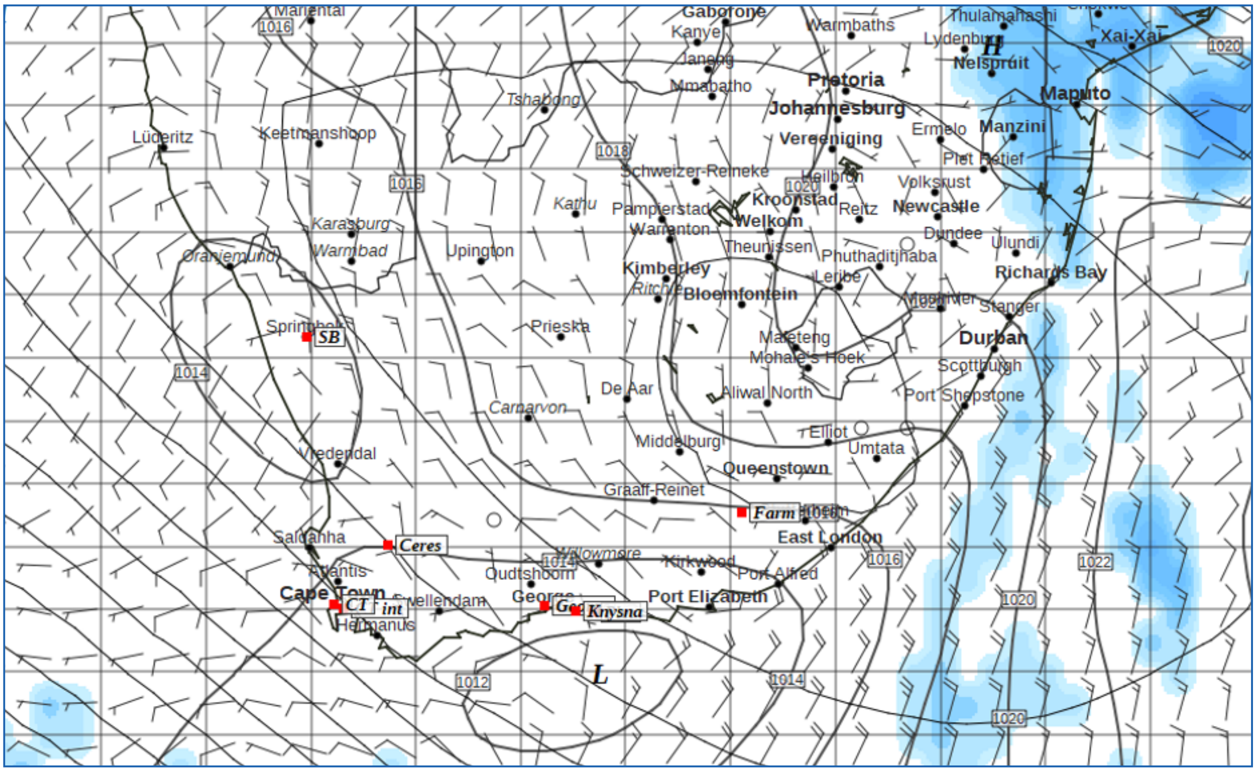

Figure 1: Atmospheric weather circulation for 4 March 2020 with the surface system indicated by the dark thick black lines and upper-air circulation as represented by the thin black lines. This indicates a surface trough dominating over the country with the coastal low over the west coast.

The aim of this study is to investigate the variation between the forecasted temperature using the different set of models with the observed temperature for 4 March 2020 over the eastern parts of the south coast and to determine how this can be used to improve our forecasting skill for maximum temperatures along the south coast when a coastal low dominates.

Forecasting temperatures for the Cape Town Weather Office usually requires one to use a set of different models and by comparing to the previous climate statistic and apply a bias correction from historical data to determine the best possible temperature forecast. On this day, looking at the model data set as well as the historical data, it is evident that model bias correction is usually +2/3°C, therefore the expected maximum temperature should be about 29 to 30°C for George and about 36°C for Knysna with the expected atmospheric condtions. However, the observed temperature for George and Knysna were about 6°C warmer than forecasted, thus resulting in an incorrect temperature forecast by a wide margin.

George 68828										30	Knysna 68935									31
Minimum				15	Maximum				24		Minimum				16	Maximum				28
UM	UC	AM	PM	Act	UM	UC	AM	PM	Act	850	UM	UC	AM	PM	Act	UM	UC	AM	PM	Act
15	12	13	13	11	21	23	24	24	25	16	15	13	16	16	13	22	29	29	29	31
16	13	14	14	15	22	23	23	23	25	13	15	14	16	16	16	23	27	25	25	30
19	15	17	17	14	22	23	25	25	26	X	19	17	18	18	17	26	31	30	32	32
17	15	16	16	17	25	27	31	31	38	23	17	16	17	17	18	29	35	36	36	42
18	15	17	17	17	22	25	25	25	25	18	19	18	18	18	18	23	29	28	28	29
X	X	18	18	19	X	X	32	32	30	23	X	X	18	18	19	X	X	36	36	37
19	18	20	20	21	25	30	37	37	31	24	19	19	20	20	21	28	38	40	40	35
19	19	21	21	18	21	26	25	25	23	15	20	20	21	21	20	21	31	27	27	27
19	20	16	16	17	20	26	23	23	21	10	19	19	18	18	18	20	32	25	25	25
19	18	17	17	17	21	27	25	21	22	11	18	19	18	18	18	21	30	27	24	24
19	18	17	17	16	21	26	21	21	23	13	18	18	18	18	19	22	30	28	28	26
19	18	16	16	16	23	27	23	23	25	14	19	19	19	19	18	26	33	31	31	32
19	17	16	16	15	23	26	24	24	25	17	19	19	18	18	16	23	28	28	28	30
19	16	15	15	17	21	24	24	24	23	17	19	19	17	17	17	21	25	25	25	28
19	16	17	17	17	20	22	20	20	19	8	19	18	17	17	18	20	25	21	21	20
18	16	16	16	15	21	23	23	23	21	8	17	16	17	17	16	22	29	25	25	25
16	14	15	15	13	23	26	27	27	28	20	17	15	16	16	15	25	30	28	28	31
X	X	15	15	15	X	X	25	25	25	13	X	X	16	16	16	X	X	26	26	27
X	X	14	14	16	X	X	25	25	23	15	X	X	15	15	18	X	X	26	26	27
X	X	17	15	15	X	X	24	23	23	14	X	X	18	18	16	X	X	26	25	27
16	14	16	16	15	19	20	23	23	23	11	16	15	16	16	15	20	*	23	23	26
15	12	15	15	14	19	20	23	23	23	15	15	14	15	15	14	20	23	24	24	26
16	14	16	16	15	20	22	22	23	23	12	15	14	15	15	17	21	25	24	25	25
16	14	15	15	13	20	22	22	22	23	12	17	16	17	17	16	20	26	25	25	27
16	14	15	15	12	21	24	24	24	25	17	15	14	16	16	13	21	27	28	28	27
14	11	10	10	11	17	20	20	20	17	3	15	14	13	13	12	18	23	22	22	20
13	10	10	10	8	19	22	22	22	19	8	13	11	11	11	9	20	26	25	25	23
14	11	15	15	9	22	25	24	24	25	X	12	11	15	15	10	21	*	26	26	27
14	11	12	12	14	19	21	21	21	21	X	14	12	12	12	16	19	22	22	22	25
14	10	11	11	10	19	21	23	23	21	X	13	12	12	12	11	19	22	24	24	24
14	11	12	12	12	19	22	22	22	21	X	12	11	13	13	13	19	23	23	23	20

Figure 2: Temperature forecast using a set of models and using the previous days and the observed temperatures for the previous months.

Wind speed and wind direction play an important role in determining the temperatures. Northerly winds bring about warm air from the interior, causing a berg wind effect for a couple of hours and influencing the temperature. On this day, north-westerly and north-easterly winds were observed and brought about an offshore air flow leading to the expected effect, but increasing the temperatures more than anticipated. Using the meteotable (GFS model) it depicted that an early maximum was expected on this day and a drop in temperature was going to set in with the later onshore flow of cooler maritime air.

Wed 2020-03-04							
⇑ 04:19 UTC ⇓ 17:01 UTC ⇑ 13:05 UTC ⇓ 23:13 UTC 61%							
00:00 UTC	03:00 UTC	06:00 UTC	09:00 UTC	12:00 UTC	15:00 UTC	18:00 UTC	21:00 UTC
276 ° 5.3 kts 2 Bf	329 ° 2.9 kts 1 Bf	8 ° 5.5 kts 2 Bf	234 ° 3.3 kts 2 Bf	207 ° 6.3 kts 2 Bf	236 ° 4.4 kts 2 Bf	321 ° 4.3 kts 2 Bf	328 ° 1.4 kts 1 Bf
6.5 kts	3.9 kts	6.9 kts	5.6 kts	7.5 kts	5.7 kts	5.2 kts	2.2 kts
0.00 mm/h	0.00 mm/h	0.00 mm/h	0.00 mm/h	0.00 mm/h	0.00 mm/h	0.00 mm/h	0.00 mm/h
4.0°C	5.8°C	9.8°C	14.3°C	5.9°C	5.2°C	6.9°C	8.5°C
21.0°C	21.9°C	25.3°C	30.0°C	23.8°C	22.7°C	21.8°C	22.2°C
17.0°C	16.1°C	15.5°C	15.7°C	17.9°C	17.5°C	14.9°C	13.6°C
5393 m	5295 m	5185 m	5103 m	5156 m	4389 m	4420 m	4473 m
1012.2 hPa	1012.5 hPa	1012.4 hPa	1012.6 hPa	1011.5 hPa	1011.6 hPa	1014.3 hPa	1016.7 hPa
9.9 %	9.0 %	11 %	7.7 %	12 %	21 %	38 %	38 %
13 %	12 %	10 %	8.2 %	10.0 %	12 %	11 %	9.8 %
8.9 %	7.6 %	9.1 %	12 %	11 %	10 %	25 %	20 %
11 %	16 %	25 %	28 %	36 %	95 %	93 %	83 %
40 %	44 %	54 %	62 %	64 %	55 %	50 %	56 %
32 %	28 %	24 %	28 %	31 %	32 %	41 %	37 %
37 %	33 %	23 %	21 %	31 %	57 %	37 %	25 %
78 %	70 %	55 %	42 %	71 %	74 %	65 %	59 %
22.6°C	23.2°C	23.8°C	23.8°C	24.5°C	24.2°C	20.6°C	21.2°C
-4.2°C	-4.5°C	-4.5°C	-4.9°C	-4.2°C	-3.7°C	-5.8°C	-5.8°C

Figure 3: Meteotable for George showing light northerly to north-easterly wind, with an early maximum, and the temperatures dropping once the winds become onshore SAST = UTC +2).

The model skew-T/ log-P graph can be used as another method to determine George's maximum temperature as depicted in Figure 4. This can be done by finding the temperature at the warmest point of the inversion (since the inversion layer is present) and proceeding dry-adiabatically from that point to the surface. The possible resultant maximum temperature forecast was about 36°C which is within 2°C of the observed temperature.

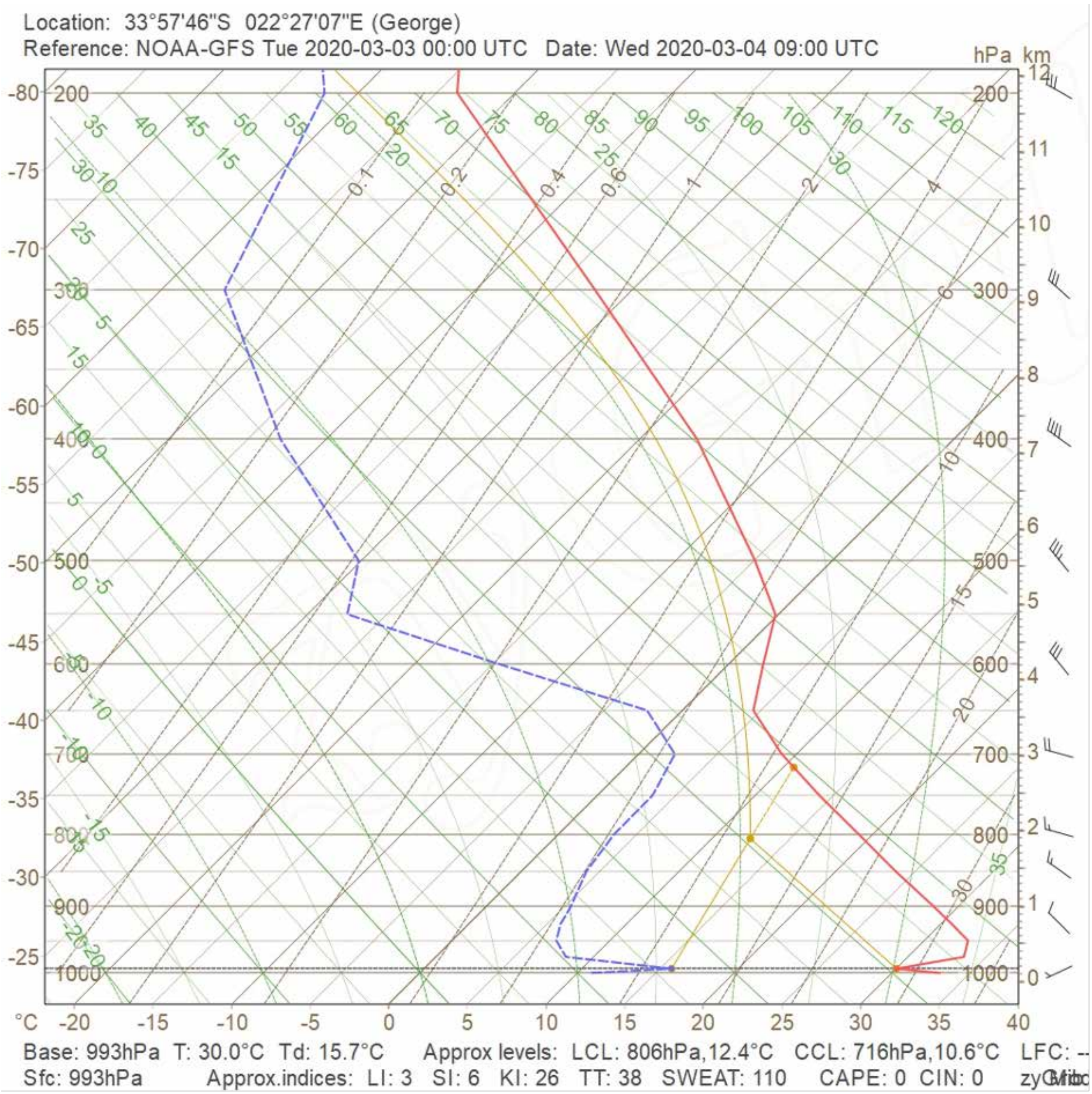

Figure 4: Skew-T/ log-P graph that shows the atmospheric profile of George, which indicates dry conditions and very hot temperatures that can be expected. By using the skew-T/ log-P graph, the possible maximum temperature should be about 35 to 36°C.

Climate statistics have proven to be of significant assistance when forecasting temperatures and on this day, using this approach would have improved the forecasted temperature. The average high maximum temperature for George was 39.9℃ and the forecasted maximum using the GFS skew-T/ log-P graph was approximately 36℃, therefore forecasting a maximum of 38℃ would be a more accurate approach to be within the 2℃ temperature range, which is the accepted margin for an accurate temperature forecast.

List: Monthly Temperature Averages and Extremes

South African Weather Service

Mean data March

	Ave Min Temp	Ave Max Temp	Ave Low Min	Ave HighMin	Extr Low Min	Extr High Min	Ave Low Max	Ave High Max	Extr Low Max	Extr High Max
Alexander Bay	14.5	23.9	10.2	19.3	7.6	25.3	21.1	33.0	16.7	41.2
Springbok	16.7	28.5	8.7	23.9	4.4	29	19.2	35.3	9.8	37.6
Calvinia	12.2	29.1	5.2	20.0	1.6	24.8	18.9	36.0	9.3	40
Sutherland	7.1	24.9	0.1	14.5	-3.3	18.2	15.0	31.4	6.2	35.1
Vredendal	14.2	30.1	8.7	20.8	6	26.2	22.5	39.9	18.2	44.8
Clanwilliam	15.9	33.0	10.3	23.3	9.2	30.1	22.6	40.7	16.1	43.4
Langebaanweg (68714)	14.1	27.3	9.0	19.8	6.8	25	20.2	36.2	15.5	40.1
Geelbek (68811)	10.8	25.8	4.7	17.5	2	23.6	20.7	34.5	15.7	37.5
Malmesbury	13.7	29.3	7.4	20.1	4.6	26.4	21.5	37.6	16.7	40.9
Paarl	16.0	29.8	10.8	21.6	9.4	25.1	22.0	37.8	17.9	41.3
Cape Town (68819)	17.3	26.3	12.7	22.9	11.3	26.1	18.8	35.7	17.3	37
Cape Town Int.	14.4	25.6	8.0	18.5	4.6	20.5	19.6	33.5	13.9	~~40.7~~
Strand	16.7	25	-	-	-	-	-	-	-	-
Slangkop	14.2	21.8	10.9	17.4	9.8	19	16.9	28.9	16.1	32.2
Cape Point	15.0	21.6	10.8	18.1	1.9	23.5	17.0	29.3	13.8	38.4
Hermanus	15.5	22.6	11.6	18.6	9.7	20.9	18.2	29.1	16.3	31.3
Grabouw	24.3	11.1	-	-	-	-	-	-	-	-
Still Bay	15.3	24.1	10.7	19.2	8.5	21.1	18.7	33.3	16.4	38
Riversdale	15.0	27.1	-	-	5	25	-	-	16	43.7
George	14.3	23.8	8.7	20.8	6.2	25	22.5	39.9	14	41.1
Robertson	14.5	28.5	7.9	20.0	4.7	21.6	19.5	37.4	15.7	40.7
Worcester	15.4	29.5	10.3	19.7	7.3	22	21.2	37.4	17.4	40.5
Beaufort West	14.3	28.6	7.8	22.1	3.5	27	18.1	36.6	12.5	39.6
Oudtshoorn	14.7	29.7	8.3	20.9	4.9	24.6	20.0	38.9	15.9	43
Excelsior	10.8	27.2	5.2	16.2	3.2	22.2	18.5	33.5	13.2	36.6

Figure 4: Monthly temperature averages and extremes for March – a useful resource to use when forecasting daily temperatures.

Preliminary findings

Looking at George's observations from METARs, it is evident that an early maximum temperature occurred on that day. It is interesting to also note that there was a sharp increase in temperature of about 5°C between 07 and 08Z, due to the north-westerly warm air from the interior. It is also clear that when winds changed to a southerly direction, the temperatures dropped significantly, with a temperature change of about 8°C.

FAGG 040400Z 03005KT CAVOK 20/17 Q1011=

Date: 2020-03-04 - **Time:** 04:30 **(Packtime: 2020-03-04 04:30)**

FAGG 040430Z 03004KT CAVOK 23/16 Q1011=

Date: 2020-03-04 - **Time:** 05:00 **(Packtime: 2020-03-04 05:00)**

FAGG 040500Z 20007KT CAVOK 21/17 Q1011=

Date: 2020-03-04 - **Time:** 05:30 **(Packtime: 2020-03-04 05:30)**

FAGG 040530Z VRB02KT CAVOK 22/18 Q1012=

Date: 2020-03-04 - **Time:** 06:00 **(Packtime: 2020-03-04 06:00)**

FAGG 040600Z 32003KT CAVOK 26/19 Q1012=

Date: 2020-03-04 - **Time:** 06:30 **(Packtime: 2020-03-04 06:30)**

FAGG 040630Z VRB02KT CAVOK 30/17 Q1012=

Date: 2020-03-04 - **Time:** 07:00 **(Packtime: 2020-03-04 07:00)**

FAGG 040700Z 22004KT 200V260 CAVOK 30/19 Q1012=

Date: 2020-03-04 - **Time:** 07:30 **(Packtime: 2020-03-04 07:30)**

FAGG 040730Z 32006KT 290V350 CAVOK 34/17 Q1012=

Date: 2020-03-04 - **Time:** 08:00 **(Packtime: 2020-03-04 08:00)**

FAGG 040800Z 34009KT 320V020 CAVOK 35/15 Q1012=

Date: 2020-03-04 - **Time:** 08:30 **(Packtime: 2020-03-04 08:30)**

FAGG 040830Z 32010KT 300V360 CAVOK 37/14 Q1012=

Date: 2020-03-04 - **Time:** 09:00 **(Packtime: 2020-03-04 09:00)**

FAGG 040900Z 29005KT 230V330 CAVOK 38/14 Q1012=

Date: 2020-03-04 - **Time:** 09:30 **(Packtime: 2020-03-04 09:30)**

FAGG 040930Z 30013KT 280V340 CAVOK 38/12 Q1012=

Date: 2020-03-04 - **Time:** 10:00 **(Packtime: 2020-03-04 10:00)**

FAGG 041000Z 22007KT 180V300 CAVOK 36/17 Q1012=

Date: 2020-03-04 - **Time:** 10:30 **(Packtime: 2020-03-04 10:30)**

FAGG 041030Z 20013KT CAVOK 28/18 Q1012=

Date: 2020-03-04 - **Time:** 11:00 **(Packtime: 2020-03-04 11:24)**

FAGG 041100Z 19014KT CAVOK 25/17 Q1012=

Figure 5: Half-hourly meteorological aerodrome reports for the George station between 04 to 11Z.

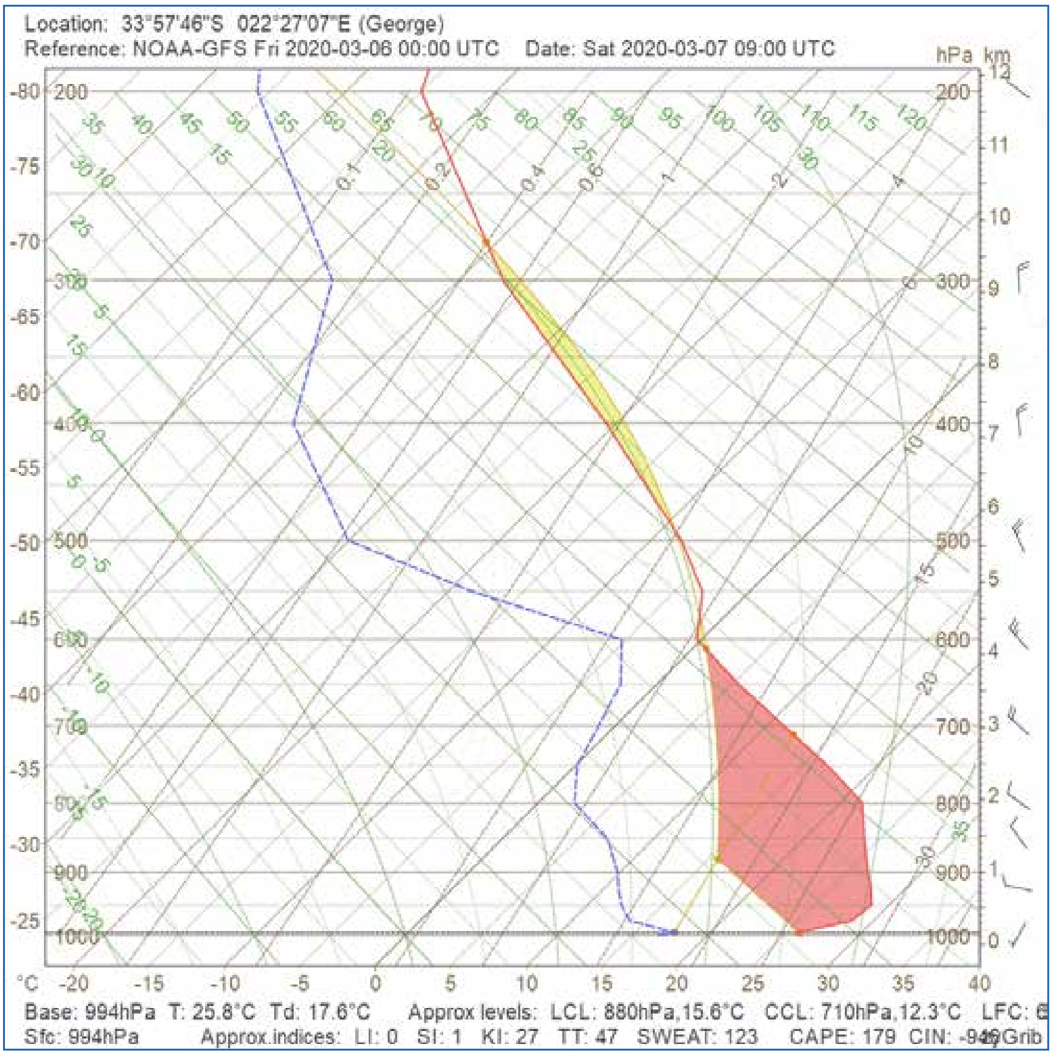

Figure 6: A skew-T/ log-P graph of for George for 7 March 2020 which had the similar atmospheric conditions as those of 4 March 2020.

Conclusion

It is important for a forecaster to understand the type of atmospheric circulation that is dominating the area of interest. If there is a coastal low present along the coastal regions, there is a high likelihood that there would be berg wind conditions, thus increasing the temperatures sharply. With coastal lows, it is advised that a forecaster should always try to determine the temperature by using the skew-T/ log-P graph as once again proven by the two days of the case study. By referring to the meteotable (GFS model) a forecaster can determine the time of occurrence of the maximum temperatures, which can also be used in other forecasting products such as Terminal Aerodrome Forecasts (TAFs). It also important to always keep at hand the historical temperature data (monthly temperatures, averages and extremes) that can assist with the temperature forecast.

References

https://www.meted.ucar.edu/mesoprim/skewt/navmenu.php?tab=2&page=2-2-1&type=flash

https://rmets.onlinelibrary.wiley.com/doi/abs/10.1002/j.1477-8696.1964.tb02714.x

http://met.dgf.uchile.cl/~rgarreau/PUBS/clow_case_MWR.pdf

https://open.uct.ac.za/bitstream/handle/11427/14293/thesis_sci_1987_heydenrych_clive_malcolm.pdf?sequence=1&isAllowed=y

http://www.cmar.csiro.au/e-print/internal/reason_x1990a.pdf

https://rmets.onlinelibrary.wiley.com/doi/pdf/10.1002/j.1477-8696.1964.tb02714.x

https://open.uct.ac.za/bitstream/handle/11427/14293/thesis_sci_1987_heydenrych_clive_malcolm.pdf?sequence=1&isAllowed=y

https://rmets.onlinelibrary.wiley.com/doi/abs/10.1002/qj.49706226707

Endurance22 expedition and finding the Endurance wreck

By Dr Tamaryn Morris

More than 100 years ago, Sir Ernest Shackleton's ship, the *Endurance*, became trapped in pack ice in the Weddell Sea off Antarctica and sank to the sea floor. The notable Antarctic explorer, having already lost out to Roald Amundsen to be the first to reach the geographic South Pole, was attempting to be the first person to cross Antarctica over land and across the pole. The hopes of the great Trans-Antarctica Expedition as it was known ended with the loss of the *Endurance*, but not the loss of life, thanks to the heroic exploits of Sir Shackleton, who saw his crew safely to Elephant Island and eventually Chile.

In February and March 2022, the Endurance22 Expedition, onboard the South African ice-breaker SA Agulhas II, was looking to be the first to rediscover the wreck of the *Endurance* in over 3000 m of water. The expedition made use of state-of-the-art technology to survey the site of the wreckage to ensure protection, but also to understand of the impact of sea ice and frigid waters on such historical artefacts.

Naturally, such an expedition to explore a remote and hostile environment offered marine scientists unprecedented access to unique data acquisition opportunities. A team from the SAWS Marine unit, Mr Marc de Vos and Ms Carla Ramjukadh, joined the vessel on 5 February 2022 to deploy ocean observing instrumentation (Argo floats, Spotter wave buoys and weather drifting buoys), undertake crucial sea ice validation experiments for the continued development of the unit's sea-ice forecasting tool, and undertake synops and upper-air measurements in support of the expedition. Their work was supported by Dr Michael Barnes and Ms Tania Daniels through a bespoke weather and ocean condition forecasting portal, which made use of UM4.4, ECMWF, GFS and ICON atmospheric forecast products, and SWaSS and Copernicus Marine Environment Monitoring Service (CMEMS) ocean products. In addition, point forecasts had been created for the port limitations of Cape Town harbour, and also for the site of the *Endurance* wreck for use by the Master and his team for safe operations.

In addition, Dr. Tammy Morris, in conjunction with Thomas Mtontsi from the SAEON Egagasini Node and the Reach the World organisation in the US (https://www.reachtheworld.org/), worked with with nine schools within both the US and South Africa to adopt, name and track the Argo floats deployed from the expedition. Due to the health pandemic, schools are no longer able to visit the vessel or preparation workshops at East Pier to learn first-hand about ocean observing technologies. However, through the international collaborations established through the expedition, opportunities arose to link schools together, with technology that allowed near-real time access to what happened on-board the vessel, including all the science and exploration activities. This gave learners first hand access to the incredible world of ocean science and technology.

The Endurance22 expedition could be followed as those on board deployed instrumentation, studied the sea-ice and explored the seafloor around the *Endurance* wreck site to become eventually become the first to rediscover this incredible piece of history. See https://endurance22.org/ and https://endurance22.org/endurance-is-found for a full account of this incredible adventure.

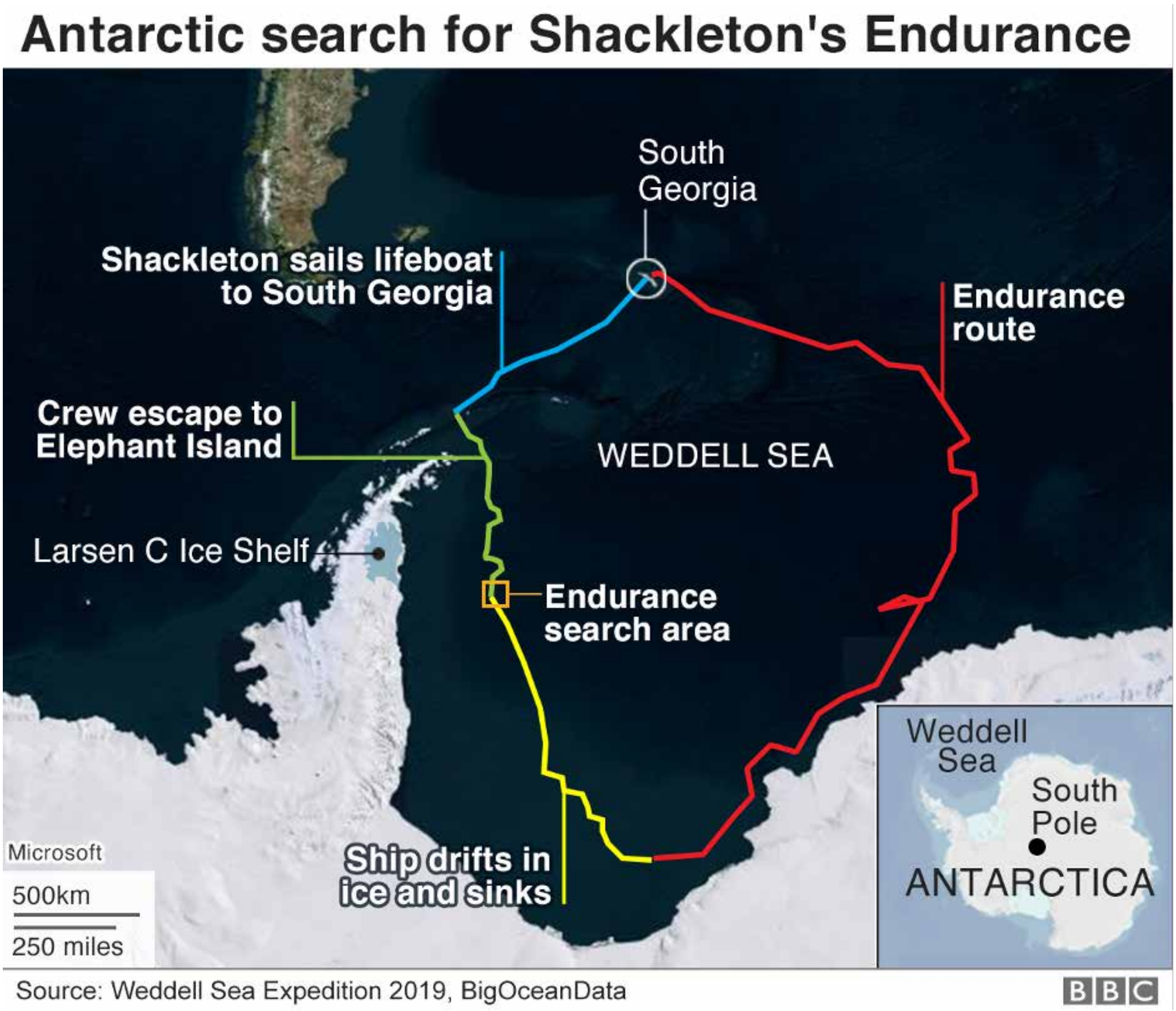

Figure 1: A map depicting the Endurance's ship track (source: BBC)

Figure 2: The Marine unit Endurance22 expedition metocean support page

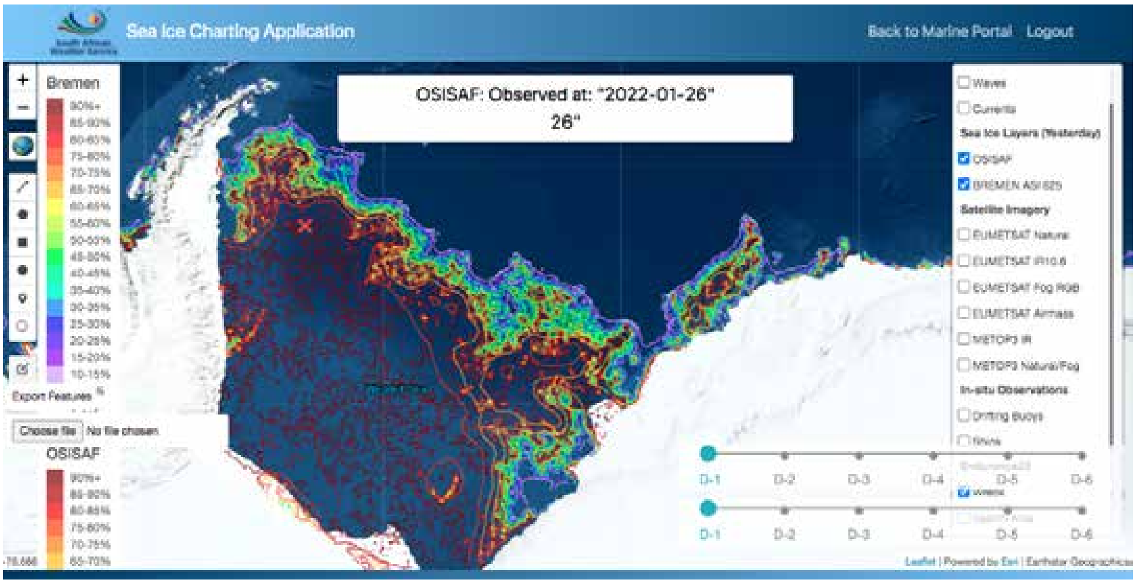

Figure 3: An example of the marine unit sea ice charting portal showing sea ice thickness from the Bremen and OSISAF products over the Weddell Sea and the wreck site (red cross) for on January 2022.

After weeks of searching on board the SA Agulhas II, the expedition team has located, surveyed and photographed the wreckage of The Endurance, Sir Ernest Shackleton's ship, which was trapped in sea ice and sunk nearly 106 years ago. The cold water and lack of wood-eating organisms has preserved this wreckage, found in an upright and proud position on the seafloor nearly 3000 m deep. Our SAWS team onboard, Marc de Vos and Carla Ramjukadh, played an instrumental role supporting the expedition in terms of weather observations and upper air ascents, along with sea ice and meteorological climatologies compiled specifically for the region, with additional support from the Cape Town Weather Office for aviation forecasts. We are incredibly proud to be a part of his historic expedition and look forward to the documentaries that will be produced through National Geographic.

Aft rail and ship's wheel, aft well deck. Image © Falklands Maritime Heritage Trust / National Geographic

Carla Ramjukadh getting ready to deploy a weather balloon from the SA Agulhas II Endurance22 expedition. Photo credit: Esther Horvath / Falklands Maritime Heritage Trust

To follow the story and for more information, please go to: https://endurance22.org/

Sources acknowledged:

https://goo.gl/LIrlur
https://www.youtube.com/c/HistoryHit
https://www.youtube.com/c/WonderDocs/featured

Shock wave effects on Automatic Weather Station (AWS) pressure readings over South Africa

By Kevin Ingram and Pumla Goba

Ben-Dor, Igra and Elperin (Ben-don, Igra, Elperin, 2001) define shock waves, in the Handbook of Shock Waves volume 2 as mechanical waves of finite amplitudes, which arise when matter is subjected to rapid compression. Additionally, they characterize shock waves by four unusual properties: (1) a pressure-dependent supersonic velocity of propagation; (2) the formation of a steep wave front with abrupt changes of all thermodynamic quantities; (3) for nonplanar shock waves, a strong decrease of the propagation velocity with distance from the origin (Hunga Tonga); (4) nonlinear superposition properties.

On 15 January 2022, the Hunga Tonga volcano erupted producing two shock waves, which proceeded to travel around the world. These shock waves produced pressure spikes around the world along the shortest route between Hunga Tonga and the AWS stations.

The shock wave was first noted on the 16th when AWS pressure data was examined, after reports of pressure spikes in Europe. Figure 1 and 2 show clear spikes in pressure for the first shock wave but a subdued spike for the second shock wave. Figure 3 shows the spikes for both shock waves very clearly in the Twee Rivieren area. The figures show that both shock waves arrived in short succession to each other, and while the second shock waves were difficult to identify on some stations, it was clearly visible on other stations.

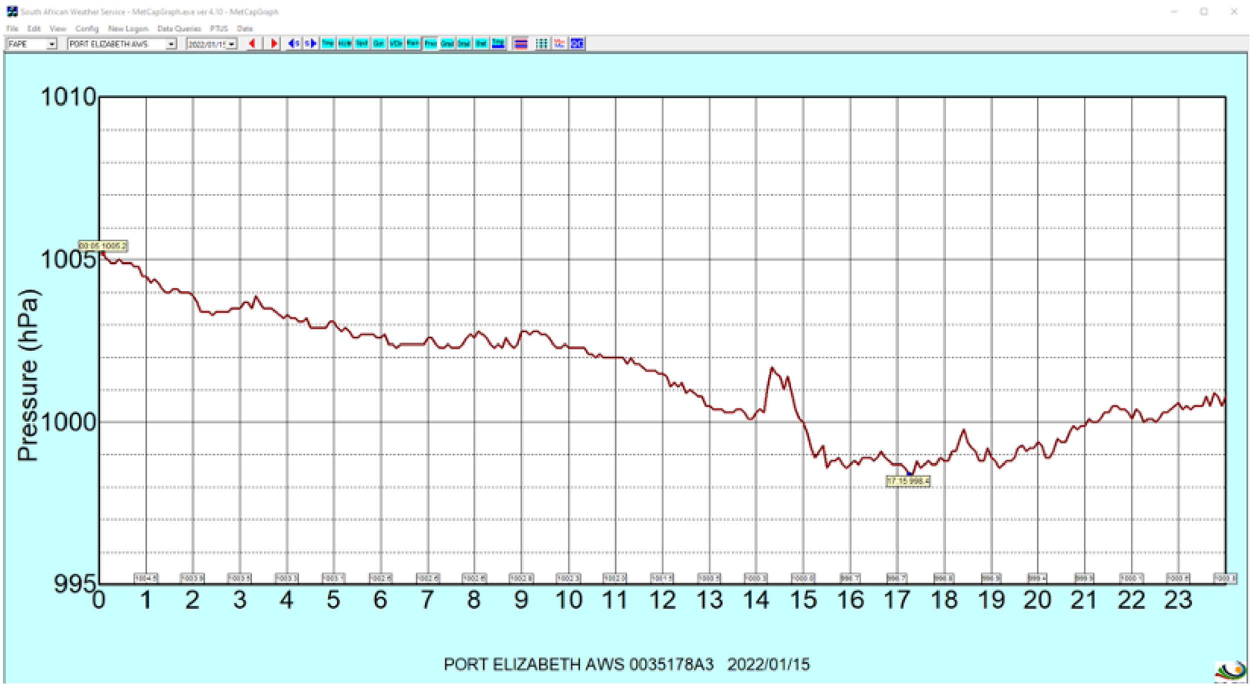

Figure 1: Port Elizabeth AWS showing a peak where the shock wave passed at 18:25 and another smaller peak at 18:55 indicating the second shock wave. The large peak after 14:00 is a result of a thunderstorm passing to the north.

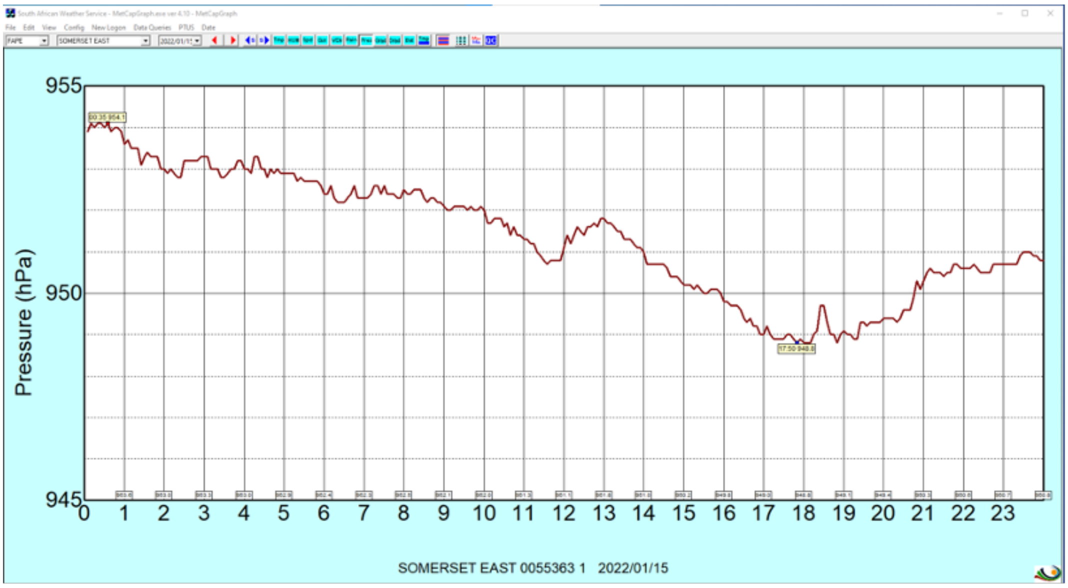

Figure 2: Somerset East AWS showing a peak where the shock wave passed at 18:25 and another smaller peak at 19:00 indicating the second shock wave.

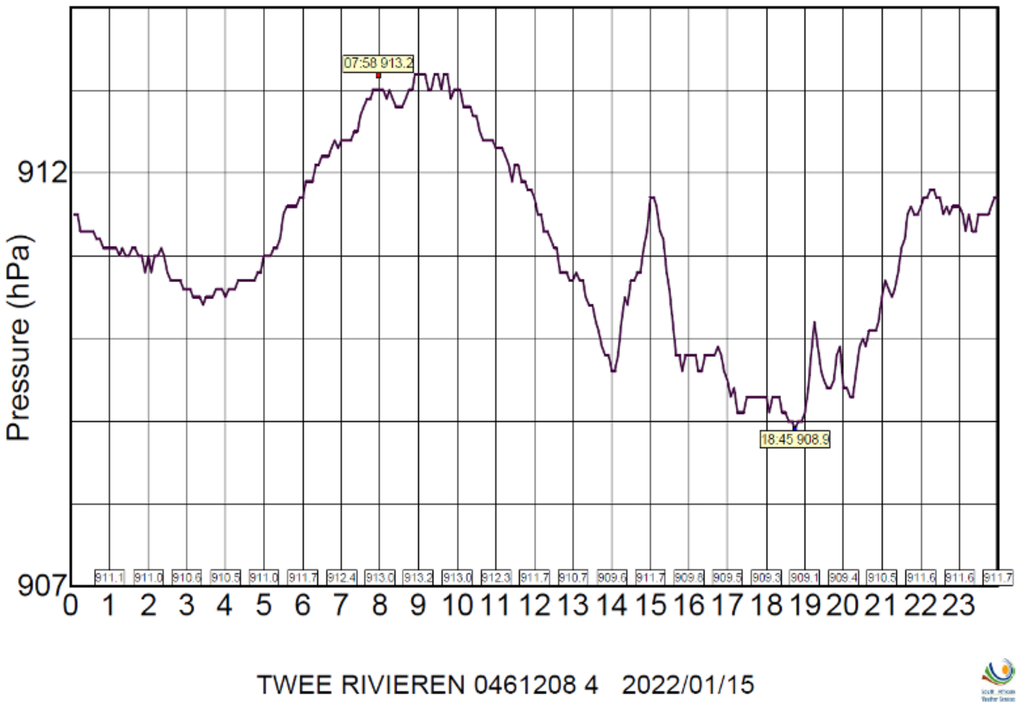

Figure 3: Twee Rivieren AWS data showing the first shockwave at 19:15 and the second shock wave at 19:55.

The Hunga Tonga shock waves arrived in short succession with the average speed of the first being slightly higher that the second. Time of arrival shows that the shock wave travelled from the south of the country over Antarctica, which is the shortest route to the country. This is further evidenced by the increasing arrival times as one travels further north - see Table 1. Marion island was hit by the shock waves first, and as it travelled north, Gough Island was hit, then Port Elizabeth, and according to the chosen stations Polokwane was the last to be hit. This shows the shock waves propagated along a northward trajectory. An overall decrease in propagation velocity is also seen in accordance with the third property of shock waves.

Table 1: Average speed calculations for shock waves 1 and 2 as dictated by the shortest distance from Hunga Tonga (Google Earth), as well as the time of arrival obtained from pressure graphs at the selected stations. Travel time was obtained by subtracting the time of eruption which was 04:00Z or 06:00 SAST from time of arrival.

Station	Shortest distance from Hunga Tonga (KM)	Time of arrival for shock wave 1 (SAST)	Time of arrival for shock wave 2 (SAST)	Travel time Shock wave 1 (hours)	Travel time Shock wave 2 (hours)	Average speed of shock wave 1 (KPH)	Average speed of shock wave 2 (KPH)
Port Elizabeth	13572.55	18:25	18:55	12.42	12.92	1092.80	1050.51
Marion Island	11829.53	16:55	17:35	10.92	11.58	1083.29	1021.54
Gough Island	13097.74	18:00	18:30	12	12.5	1091.48	1047.82
Upington International Airport	14300.16	19:10	19:35	13.17	13.58	1085.81	1053.03
Polokwane	14402.83	19:50	20.15	13.83	14.25	1041.42	1010.73
Twee Rivieren	14523.27	19.10	19:55	13.25	13.92	1096.10	1043.34
Alexander Bay Airport	14419.82	19:10	19:45	13.17	13.75	1094.90	1048.71

On the 16th the shock waves were again seen on all the stations initially indicating that the shock wave had travelled around the world and returned again. However, the fact that the Twee Rivieren and Polokwane shock waves occurred before the Port Elizabeth and Somerset east shock waves would indicate that the initial shock wave dissipated and did not return a second time, instead the shock wave came from the north-east and travelled southwards. This shows that this shock wave is the one that travelled from the other side of the world and reached South Africa before dissipating.

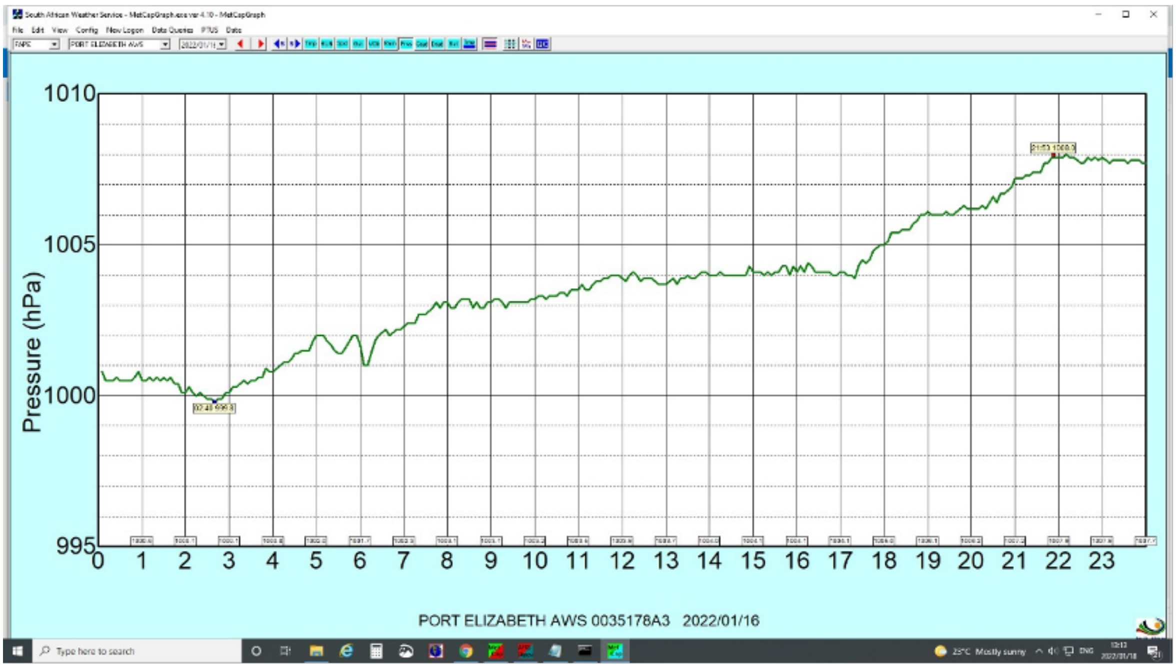

Figure 4: Port Elizabeth AWS for the 16th showing the shock waves returning at 05:00 and 05:55.

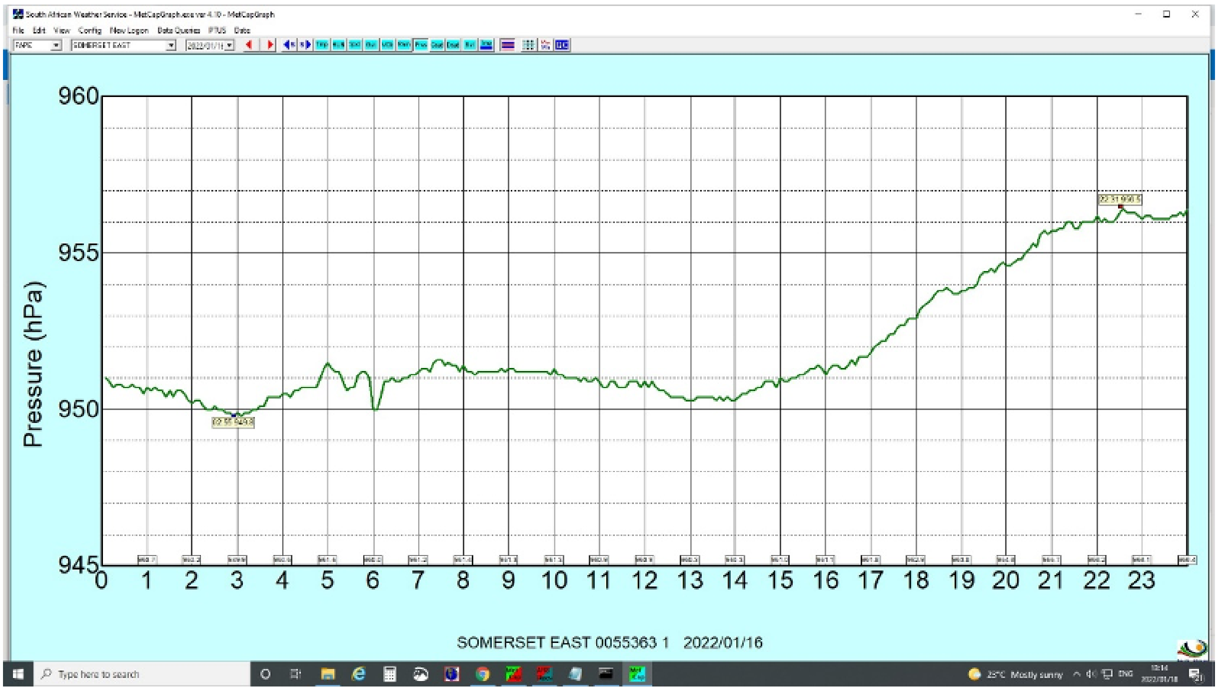

Figure 5: Somerset East AWS for the 16th showing the shock waves returning at 05:00 and 05:55.

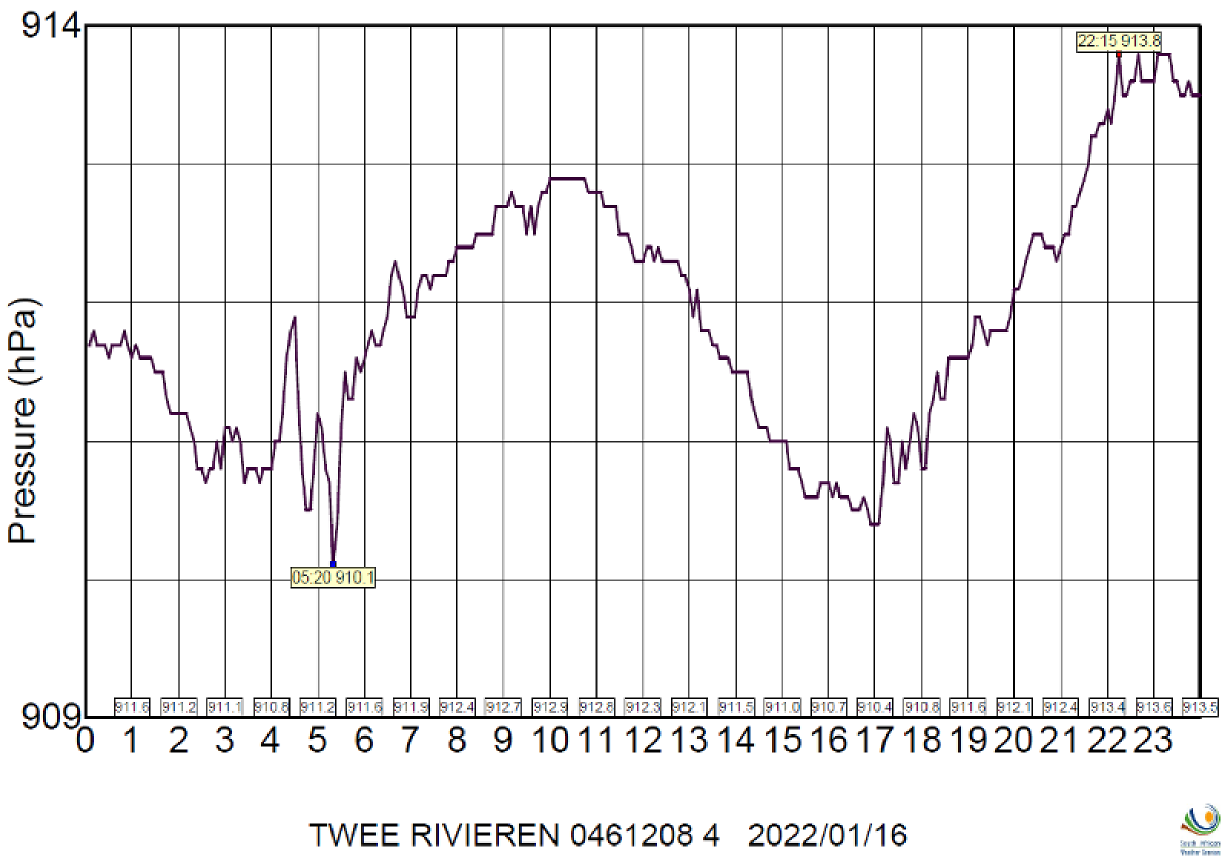

Figure 6: Twee Rivieren AWS for the 16th showing the shock waves returning at 04:30 and 05:00.

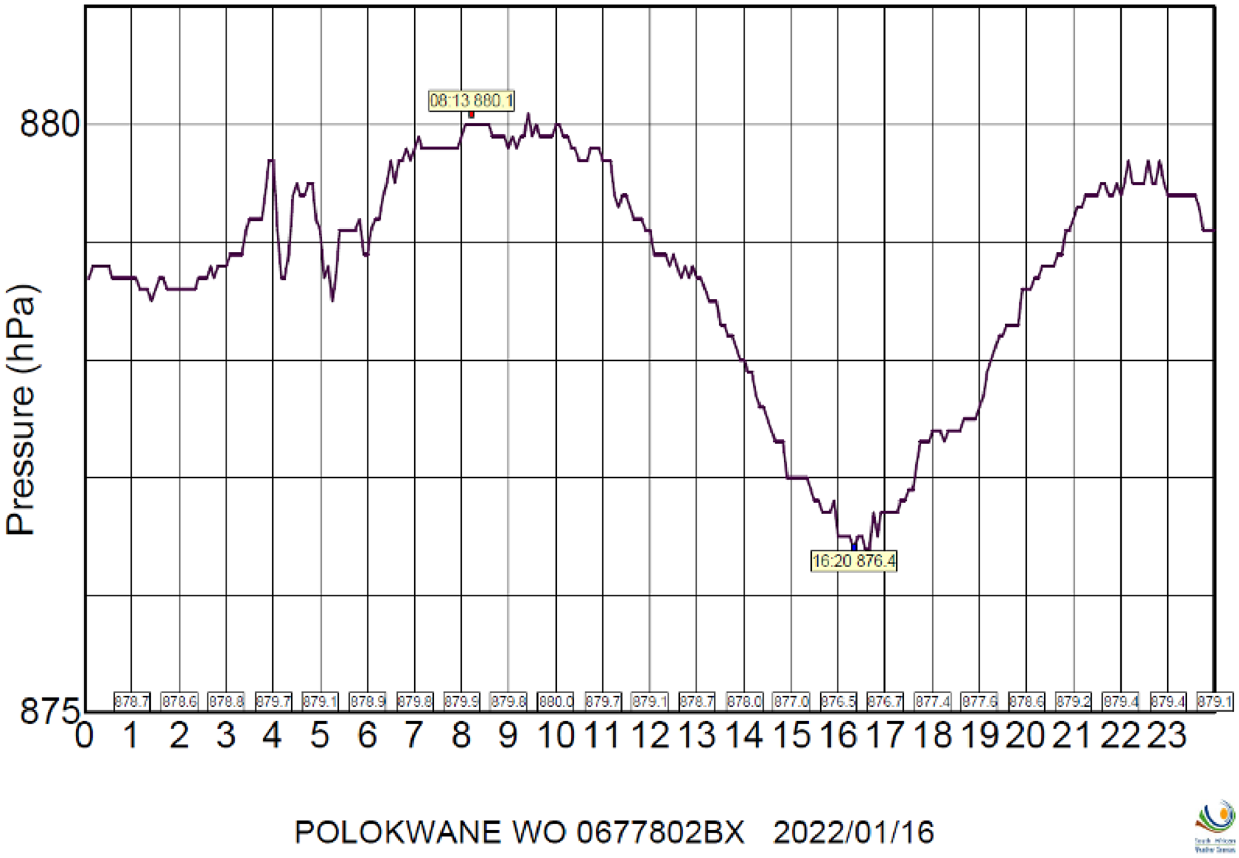

Figure 7: Polokwane AWS for the 16th showing the shock waves returning at 04:00 and 04:30.

In conclusion, we see that powerful shock waves from volcanoes can and do travel around the world causing pressure disruptions in AWS stations. These shock waves may then continue travelling after colliding at the opposite end of the world before dissipating, causing a second round of pressure spikes hours later. But we should not forget the definition of shock waves as stated by Ben-Dor, Igra and Elperin. The second property should still hold true, and therefore further research into disruptions of other parameters such as temperatures and even moisture can be done in the future.

References

Ben-Dor, G, Igra, O, Elperin, T, 2001. Handbook of Shock Waves, Three Volume Set: 2-3.

https://books.google.co.za/books?id=qcYjUc7A9KMC&printsec=frontcover&dq=shock+waves&hl=en&sa=X&redir_esc=y#v=onepage&q=shock%20waves&f=false

Meet the Authors

Lesetja Lekoloane

Mr Lesetja Lekoloane is a data scientist at the South African Weather Service, working on the Integrated Climate-driven Multi-Hazard Early Warning System. His other research focuses on model development, severe convective storms, and weather and climate dynamics. He also has an interest in applying data science techniques in the development of operational systems.

Mr Brighton Mabasa

Mr. Brighton Mabasa is a research scientist in Applications (Renewable Energy Applications and scientific consulting) at South African Weather Service (SAWS). Brighton's duties in the group includes SAWS Solar Radiometric Network monitoring and maintenance, data archiving, data quality control using Baseline Solar Radiation Network (BSRN) standards, satellite data validation, product development, observation data preparation for model verification, solar radiation and biometeorology station installation and calibration using ISO standards, writing peer reviewed articles and writing Standard Operating Procedures (SOPs) for operational activities.

Brighton Mabasa is registering for MSc in Atmospheric Physics at UNISA, research outputs will support an advanced operation of the SAWS solar radiometric network.

Mr Puseletso Mofokeng

Mr. Puseletso Mofokeng is a senior forecaster at the Disaster Risk Reduction Department of the South African Weather Service. His roles include overseeing the services which are being provided for the South African public and also generating extreme weather forecasts for all the 16 countries in the Southern Africa Development Community (SADC). Mr. Mofokeng enjoys writing and, in the recent past, he wrote about 40 columns and articles for various newspapers. Currently made a commitment to engage in rigorous masters' program at the University of Witwatersrand.

Ms Samukelisiwe Thwala

Miss Samkelisiwe Thwala is a weather forecaster who is currently based at the Cape Town Weather Office while simultaneously works as a meteorologist at the Koeberg Nuclear Power Plant. She studied both BSc and BSc (Hons) Meteorology at the University of Pretoria. She is passionate about severe weather events that affects the general public and writing case studies about such events.

Dr Tamaryn Morris

Tamaryn Morris is a Senior Scientist with the SAWS Marine Unit, based in Cape Town. She was recently awarded an NRF Y1 rating as an up and coming scientist in her field. She oversees the SAWS SANAP responsibilities and is heavily involved in ocean observing networks and deployment of instruments around South Africa.

Mr Hetisani Oscar Shiviti

Mr Hetsani Oscar Shivit is a forecaster at the Aviaton Weather Center (AWC) at OR Tambo Internatonal Airport. He completed both the BSc degree and BSc honours degree in Meteorology at the University of Pretoria. He also further completed the forecastng training provided by the South African Weather Service (SAWS) for a full year. Since his employment he has been a willing partcipant on SAWS outreach initatves to educate the public on weather related issues.

Ms Pumla Goba

Ms Pumla Goba was born and bred in one of the rural and very small areas of the Eastern Cape and therefore it was only fitting to start her forecasting career in the Eastern Cape. She completed her BSc degree in Mathematics and Applied Mathematics in 2002 at the Nelson Mandela University (formerly known as University of Port Elizabeth). She joined SAWS in 2008, working as a forecaster in Gqeberha after obtaining her BSc Honours in Meteorology at the University of Pretoria. While working as a forecaster, she managed to obtain a BSc in Applied Mathematics.

What she loves about being a forecaster is that you don't take your job home. With weather forecasting you learn new things/ techniques all the time and that gives us something to think about other than stressful things.

Mr Kevin Ingram

Kevin Ingram is a forecaster working at the Port Elizabeth Forecasting Office. Kevin completed his forecasting certificate in 2017 and joined SAWS in 2018 in the Bloemfontein Forecasting Office, and was trained and mentored most notably by Tonie Rossouw and Quinton Jacobs, where he learned valuable knowledge and the importance of a good working relationship. He worked there until 2021 when he transferred to the Port Elizabeth Forecasting Office.

Head Office

Centurion
Eco Glades
Block 1B, Eco Park
Cnr Olievenhoutbosch and
Ribbon Grass Streets
Centurion
0157

Regional Offices

Bloemfontein
Weather Office
Maselspoort Road
Bram Fisher International Airport
Private Bag X20562
Bloemfontein
9300
Tel: 051 433 3281

Cape Town International
Weather Office
ATNS Tower
Tower Street
Cape Town International Airport
PO Box 21
Cape Town International Airport
7525
Tel: 021 934 0749/0831

King Shaka International
Weather Office
Ground Floor
ATNS Building
King Shaka International Airport
PO Box 57733
King Shaka International Airport
4407
Tel: 032 436 3820/3812

OR Tambo International
Aviation Weather Centre
Room N161
3rd Floor
OR Tambo International Airport
PO Box 1194
Kempton Park
1627
Tel: 011 390 9329/9330

Port Elizabeth
Weather Office
Roof Top
Departures Hall
Port Elizabeth Airport
Private Bag X5991
Walmer
Port Elizabeth
6065
Tel: 041 581 0403/8587

WEATHERSMART NEWS

Scientific meteorological and climatological news from the South Africa Weather Service

South African
Weather Service